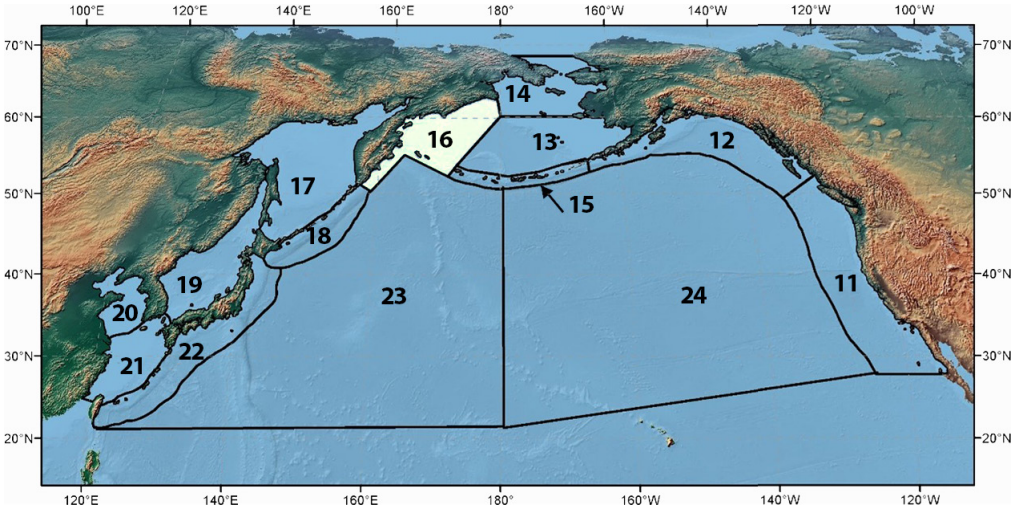

PICES

Regional Report for PICES Region:

16

PICES SPECIAL PUBLICATION 7

Marine Ecosystems of the North Pacific Ocean 2009–2016

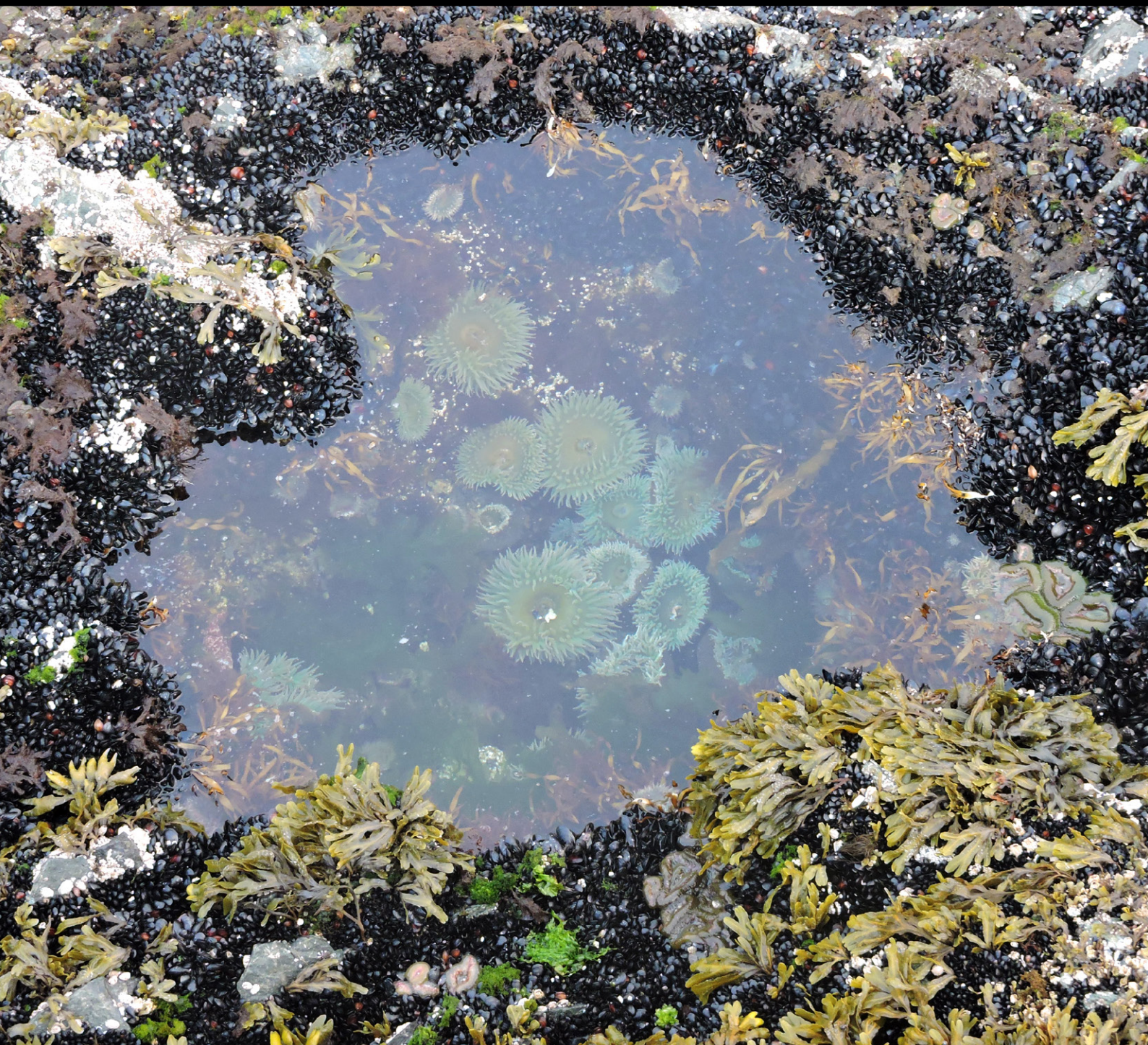

PICES North Pacific Ecosystem Status Report, Region 16 (Western Bering Sea)

Kirill K. Kivva

Russian Federal Research Institute of Fisheries and Oceanography (VNIRO), Moscow, Russia

Contributing authors:

Evgeniy O. Basyuk[1], Gennady V. Khen[1], Arseniy A. Kubriakov[2], Larisa Y. Matyushenko[1], Aleksey A. Somov[1], Natalia V. Klovach[3], Aleksander O. Zolotov[1], Marina A. Shebanova[1], Natalia A. Kuznetsova[1], Viktor A. Nadtochy[1], Nikolay V. Kolpakov[1], Mikhail V. Simokon[1], Lidia T. Kovekovdova[1]

[1]Pacific branch of Russian Federal Research Institute of Fisheries and Oceanography (TINRO), Vladivostok, Russia

[2]Marine Hydrophysical Institute RAS (MHI RAS), Sevastopol, Crimea

[3]Russian Federal Research Institute of Fisheries and Oceanography (VNIRO), Moscow, Russia

1. Highlights

The deep part of the western Bering Sea was in a generally warm state from 2003 through 2016. There were slightly negative temperature anomalies in the 50-300 m layer in 2008-2013, but this event is over and the whole upper 0-1000 m layer has been warmer than average for 1950-2000 since 2014. Salinity of the upper layer is generally decreasing in the area since at least 2003 at least in autumn.

Phytoplankton blooms occured later than previously in the area close to Cape Navarin since 2013 and earlier near Kamchatka Strait since 2009; the connection between bloom timing or its amount and physical factors is complex and non-linear.

Meso-zooplankton biomass consistently increased since 2012 mostly due to increase of chaetognaths (arrowworms) which are an important feeding resource for commercial fishes. The reason for this increase is most likely related to the warming and it may also depend in some part on changes in large scale water circulation.

According to summer-autumn surveys, the biomass of nekton has decreased in the western Bering Sea (WBS) in 2010-2015 compared to 2003-2010. There was a decrease in biomass of all dominant taxa (mostly immature salmons, squids and mesopelagic species), as well as Atka mackerel and benthic species. On the other hand, Pacific herring and southern migrants such as Pacific pomfret, Pacific saury, Pacific spiny dogfish, and Japanese anchovy were in general more abundant in 2010-2015 than in 2003-2010.

Despite the decreasing biomass of immature salmon in the upper epipelagic layer in autumns of recent years, the catches of the mature salmon consistently increased in the

region. This reflects general decrease in mortality of salmon during their oceanic migrations during winter in recent years (2004 to 2016).

A general decrease in walleye pollock catch has occurred in the WBS region in recent years. Contrarily, the catch of Pacific herring increased in the Karaginsky Gulf statistical area in 2012-2016 (this report, section 9.1. Non-salmon fisheries).

Studies of the benthic community structure of the Olyutorsky Gulf reveals the general stability of this community in terms of dominant species and their biomass although there is substantial spatial redistribution of species. The bivalve *Macoma calcarea* spread northward to the inner shelf and lost dominance in the middle shelf in the eastern part of the gulf. The sea urchin *Strongylocentrotus pallidus* became the dominant species in a narrow band of the middle shelf.

Existing information on trace metals and persistent organic pollutants in the western Bering Sea indicates this area is currently not in danger of chemical contamination.

2. Introduction

Contributor: K.K. Kivva.

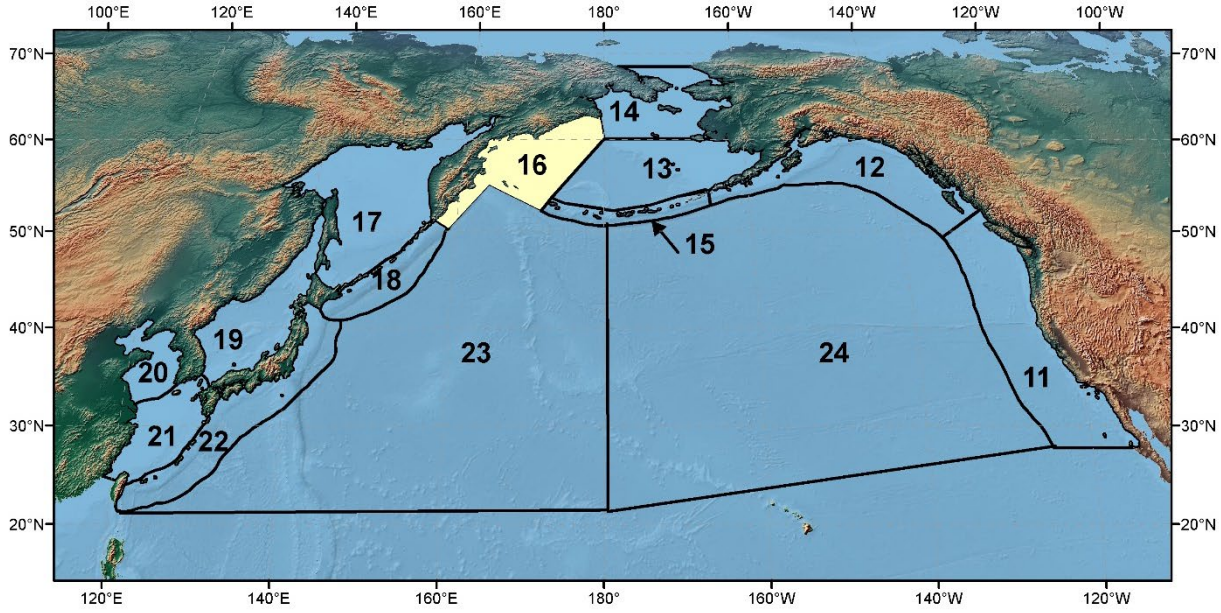

Figure R16-1. The PICES biogeographical regions and naming convention for the North Pacific Ocean with the area discussed in this report highlighted.

Several comprehensive descriptions of the Bering Sea ecosystem, its spatial organization and temporal dynamics exist in the literature. The most significant and recent of them are books “Dynamics of the Bering Sea” (Loughlin and Ohtani, 1999), Volume 10 (“The Bering Sea”) of the USSR project “Hydrometeorology and Hydrochemistry of the seas” (Terziev, 1999; note this book is available in Russian only), and PICES Special Publications 1 “Marine Ecosystems of the North Pacific” (Perry and McKinnell, 2004) and 4 “Marine Ecosystems of the North Pacific Ocean, 2003-2008” (McKinnell and Dagg, 2010; Hunt et al., 2010). However, little attention is paid in these sources specifically to the western Bering Sea. On the other hand, some other contributions are focused on processes occurring in the western

part of the sea. Those include the book “Current state of the ecosystem of the western Bering Sea” (Makarevich, 2010; in Russian) and multiple journal articles, many of which are cited in this report. The dynamics of western Bering Sea ecosystem in the most recent time interval of 2009-2016 is only in part covered in several journal articles, most of which are in Russian and not easily accessible for non-Russian-speaking readers. Moreover, despite large amounts of data on physical and chemical conditions as well as on zooplankton and fish being collected during regular oceanographic fishery surveys, information on some particular parts of the ecosystem or their dynamics is still almost entirely absent in the literature. Thus, the main aim of this report is to combine all available published information and at least some portion of existing unpublished data on the functioning and dynamics of the western Bering Sea ecosystem with a particular emphasis on the years of 2009-2016. Below we provide a brief description of the area of interest. In separate sections we describe physical (3) and chemical oceanography (4) of this area, phytoplankton dynamics there (5), review existing data on fish (7) and benthic (8) community structure and dynamics, report recent peculiarities of fishing activities in the region (9), briefly describe available data on contamination of the area (10), and provide a general conclusion (11). We pay special attention to the structure of every part of the ecosystem and describe it based on multi-year mean data when available as most of the existing sources omit this information.

The Bering Sea is the very northern part of the North Pacific. Thus, Arctic air masses largely determine its climate, and relatively free water exchange occurs between the sea and Pacific along the Commander-Aleutian Islands chain (Figures R16-1, R16-2). It is a valuable fishery region (e.g., Kotenev, 1995; Matishov et al., 2009; Belkin, 2016; Datsky, 2019a) and the only pathway for relatively warm North Pacific waters flowing into the Arctic Ocean (e.g., Baker et al., 2020; see report on the Region 14 – the Northern Bering Sea). Thus, dynamics of its ecosystems are important to consider both for economic and ecological reasons.

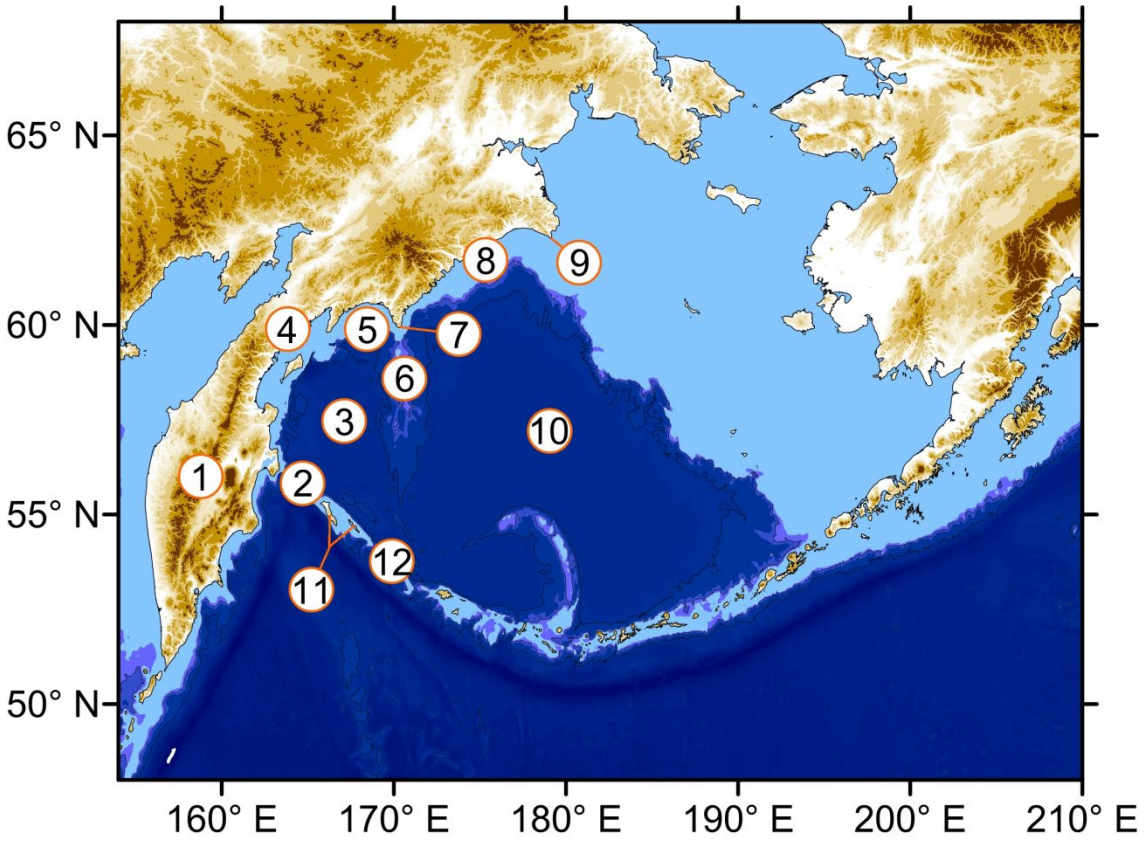

Figure R16-2. General bathymetry of the Bering Sea region based on GEBCO. Light blue color represents depth < 200 m. Numbers mark major geographic nomenclature of the western Bering Sea region: 1 – Kamchatka Peninsula; 2 – Kamchatka Strait; 3 – Kamchatka (Commander) Basin; 4 – Karaginsky Gulf; 5 – Olyutorsky Gulf; 6 – Shirshov Ridge; 7 – Cape Olyutorsky; 8 – Koryak Shelf; 9 – Cape Navarin; 10 – Aleutian Basin; 11 – Commander Islands; 12 – Near Strait.

The Bering Sea is divided into two approximately equal areas by morphological features. The eastern shelf area is wide (approximately 500 km) and shallow (<200 m), and the western part is deep with depths of more than 3500 m (Moiseev, 1963; Hood and Kelley, 1974). The western shelf is narrow compared to the eastern shelf with characteristic width of about 25-80 km (Khen, 2010). An exception is the Karaginsky Gulf where the shelf width is about 120 km. The shelf break of the western Bering Sea occurs at depth of about 90-110 m in the Kamchatka Strait and about 250-320 m in the Olyutorsky Gulf. The slope which separates deep waters from shelf areas in the western Bering Sea is relatively steep with an inclination of about 7-12° (Gershanovich, 1963). The slope width changes from 13-25 km in the very western part to 100-150 km in the north-western part of the area.

The main morphological feature of the western Bering Sea is Shirshov Ridge. The ridge spans to the south of Cape Olyutorsky for about 670 km, and the water depth above it changes from about 300 m in the north to 1500-4000 in the south. The ridge delineates the western Bering Sea into two basins: Aleutian Basin to the east, and Commander (Kamchatka) Basin to the west of the ridge.

3. Physical Oceanography

Contributors: E.O. Basyuk, G.V. Khen, K.K. Kivva, L.Y. Matyushenko.

3.1. Currents

The main currents of the Bering Sea form a cyclonic circulation along the shelf break. It includes Aleutian North Slope Current, Bering Sea Slope Current, and Kamchatka Current (Figure R16-3). This circulation spins up in cold season (January-March) and slows in summer (July-September) (Natarov, 1963; Hughes et al., 1974; Ladd, 2014). It represents the northern limb of the western subarctic gyre of the Pacific Ocean (Pickart et al., 2009) The very northern part of the Bering Sea is dominated by flows towards the Bering Strait which are strongest in summer. Mean currents on the eastern shelf are relatively weak (<5 cm s^{-1}) and generally have northward direction (Stabeno et al., 2016). As the western shelf is relatively narrow, the characteristic currents there generally mimic the currents of the adjoining deep Bering Sea. Only in the very north-eastern portion of the western Bering Sea shelf the Navarin Current flows against the Kamchatka Current. It is evident generally in summer along the Koryak Shelf.

The main changes in set-up of physical conditions of the Bering Sea are ruled by interaction of the sea with air masses of Arctic and Pacific origin, water advection from the Pacific, and redistribution of these water masses within the sea.

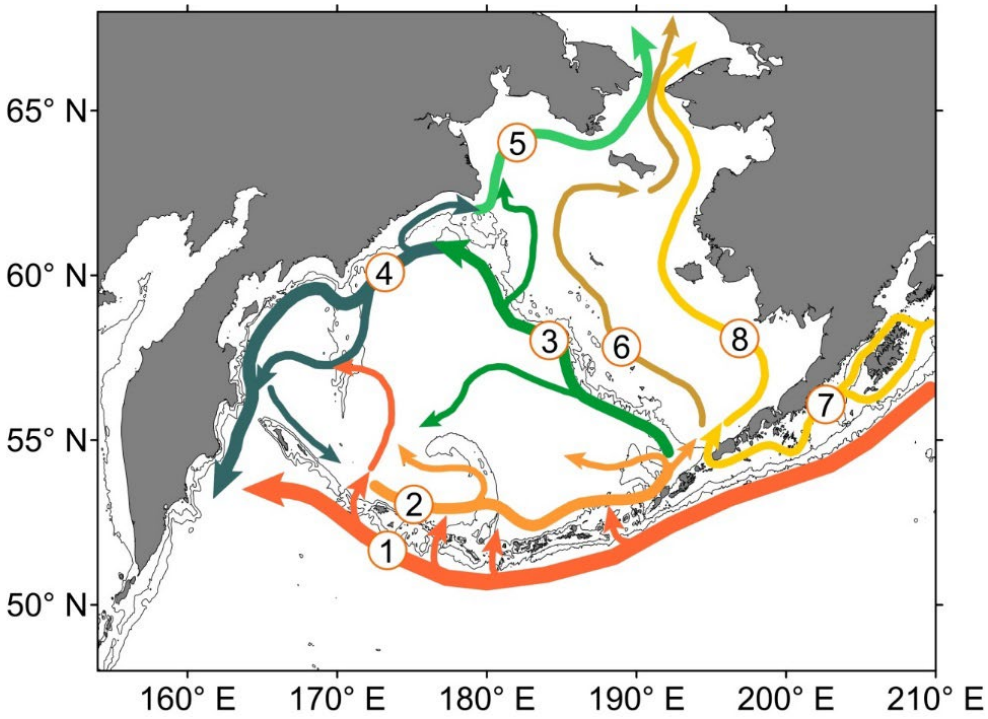

Figure R16-3. General circulation scheme of the Bering Sea region. 1 – Alaska Stream; 2 – Aleutian North Slope Current; 3 – Bering Slope Current; 4 – East-Kamchatka Current; 5 – Anadyr (Navarin) Current; 6 – flow along the eastern shelf; 7 – Alaska Coastal Current; 8 – flow of Alaska Coastal water along the shelf. Solid lines denote the 200 m and 2000 m isobaths based on the General Bathymetric Chart of the Oceans (GEBCO).

3.2. Hydrography and stratification

Characteristic vertical structure in the western Bering Sea in summer include an upper mixed layer (approximately 0-25 m), seasonal thermocline (approximately 25-55 m), cold intermediate (dichothermal) layer (approximately 55-250 m), warm intermediate layer (250-520 m), and deep Pacific water mass (Figure R16-4). Water of dichothermal layer is formed during winter season. Strong winds and thermal convection mix upper water column to 200-350 m starting in October-November. The depth of convection depends on winter heat loss, which is controlled by air temperature and wind speed. Air temperature is generally lower, and winds are stronger along the Siberian coast (Moore and Pickart, 2012). The bottom of active layer is deepest (up to 350 m) along Kamchatka Peninsula (Luchin, 2007). Thus, bottom of dichothermal layer is also lower there in summer compared to the central part of the sea (eastern part of section in Figure R16-4). The warm intermediate layer has Pacific origin. This water flows into the Bering Sea mostly through the Near Strait and propagates around the sea similar to the general surface water circulation. This water loses heat along the way, so the core of warm intermediate layer has a temperature of about 3.8-4.0 °C in the Near Strait, about 3.7-3.8 °C in the central part of the sea, and about 3.6-3.7 °C along the continental slope of the Kamchatka Basin.

Unlike temperature, salinity increases through the water column. The upper mixed layer is fresher along the coastal part of the western Bering Sea due to ice melt in spring and transport of fresher water from the north. This leads to a stronger halocline along the coastal part of the area.

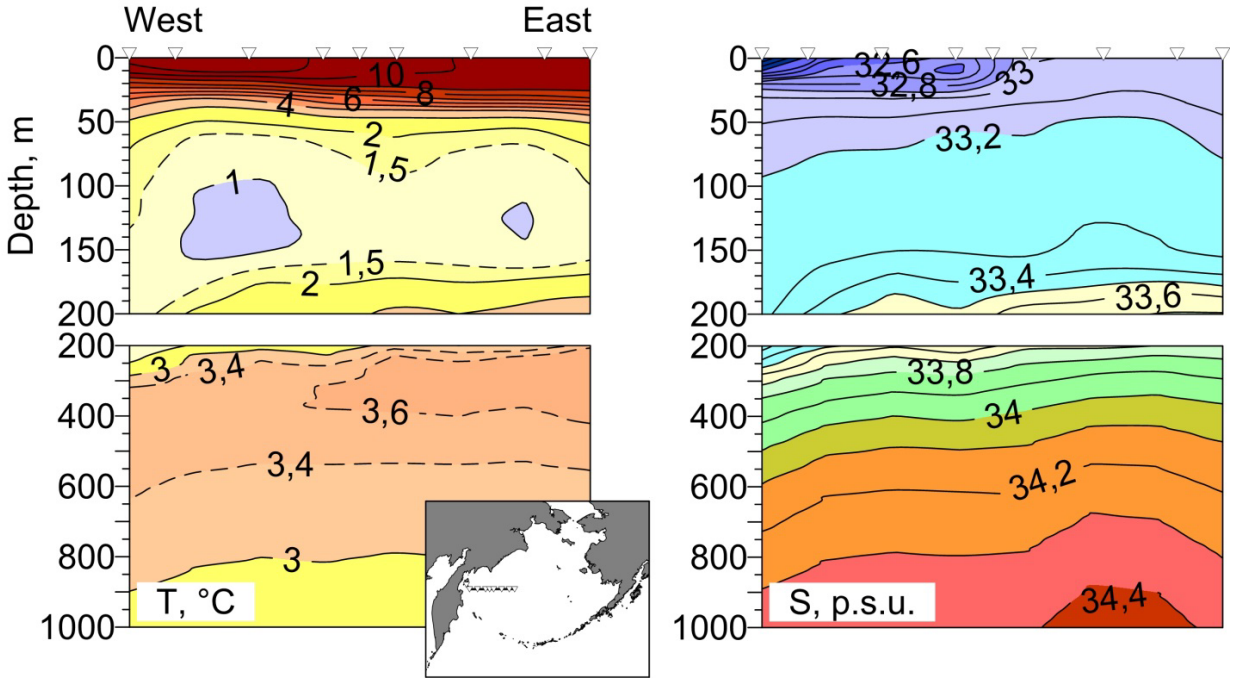

Figure R16-4. Characteristic vertical distribution of temperature, °C (left panel) and salinity, p.s.u. (right panel) in the western Bering Sea. The data is from quasi-synoptic section, August 2002. Station locations are marked with triangles (see inset map for section location).

To shed a light on water column temperature and salinity dynamics, *in situ* data should be used. We apply available cruise CTD data of the Pacific branch of the Russian Federal

Research Institute of Fisheries and Oceanography (TINRO) from June-November of 1988-2017. The data was averaged for WBS area. Despite the area being sampled in different months during different years, the data still reveal general subsurface temperature variability. However, temperature values for the upper 50 m should be analyzed with caution as seasonal heating or autumn mixing could possibly introduce some error.

Variability of salinity was assessed for the 0-50 m layer. Seasonal changes in salinity of the upper layer are quite prominent during summer-autumn. To avoid erroneous results, we limit salinity data analysis by September and October. This restricts the sampling period to 2002-2017.

Temperature anomalies (T_a) were calculated relative to the values in "Climatic Atlas of the North Pacific Seas: Bering Sea, Sea of Okhotsk, and Sea of Japan" (Luchin et al., 2009). This is gridded (1°×2° latitude-longitude) monthly climatology for 1950-2003 at standard depths. Anomalies were first calculated for every *in situ* station for standard depths, and then averaged over the area of interest. Methodological details are given in Basyuk (2011). Temperature conditions were typified using the approach of Luchin and Sokolov (2007). Standard deviation was calculated for a 30-year interval (1988-2017) for every depth ($\sigma_{1988\text{-}2017}$). T_a values were divided into five groups as follows: extremely cold ($T_a < -2\sigma_{1988\text{-}2017}$), cold ($-2\sigma_{1988\text{-}2017} \le T_a \le -0.674\sigma_{1988\text{-}2017}$), normal ($-0.674\sigma_{1988\text{-}2017} < T_a < 0.674\sigma_{1988\text{-}2017}$), warm ($0.674\sigma_{1988\text{-}2017} \le T_a \le 2\sigma_{1988\text{-}2017}$), and extremely warm ($2\sigma_{1988\text{-}}2017 < T_a$). Thus, the absolute values of T_a are related to thermal state of the second half of twentieth century, and types of thermal conditions of every year (summer data) are for the last thirty years.

Water column temperature anomalies for June-November of 1988-2017 relative to the mean of 1950-2003 are presented in figure R16-5. T_a values were generally positive during most parts of 1996-2017 in the upper 50 m layer. This means in the beginning of the twenty-first century, the upper layer of the western Bering Sea was substantially warmer than during the second half of twentieth century. Nevertheless, the dichothermal layer under the seasonal thermocline (depth range of 50-200 m) was mostly colder during the same interval than in 1950-2003. Only in 1997 and 2014-2017 did the whole active layer show positive temperature anomalies relative to 1950-2003. 1997 is the year of a strong El Niño event which probably led to anomalously warm conditions in the western Bering Sea. Contrarily, the La Niña event of 1999-2000 led to cold conditions in the whole active layer. In recent years, while the upper 10 to 50 m layer was warm or extremely warm, cold conditions were evident in the dichothermal layer in 2009-2010 and 2012-2013. In general, the dichothermal layer in the WBS had negative temperature anomalies in 2006-2013. This was mostly due to cold winters with large sea ice extent (Khen et al., 2014). After 2014, the whole 0-1000 m water column was warmer than during 1950-2003.

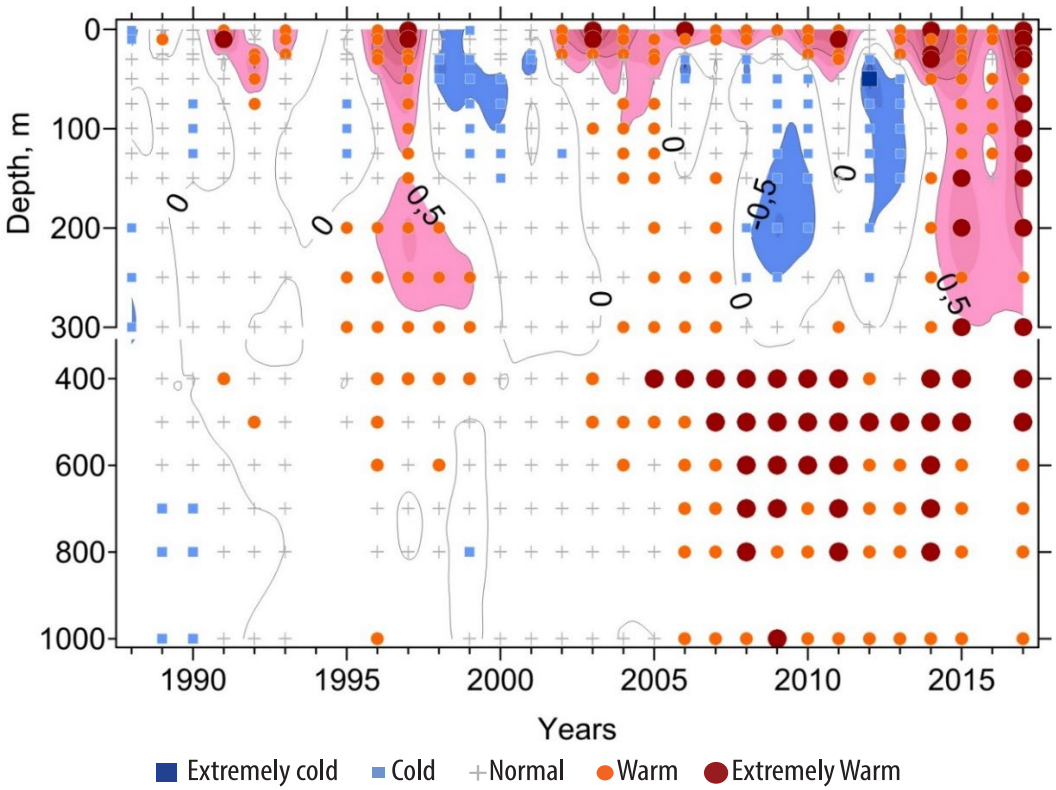

Figure R16-5. Mean temperature anomalies (T_a, units are °C, showed as isolines with shading, isolines interval is 0.5 °C) and degree of deviation of T_a from the multi-year mean (symbols, see below) in the western Bering Sea. The figure is based on data of TINRO for June-November for standard horizons relative to mean for 1950-2003 from “Climatic Atlas of the North Pacific Seas: Bering Sea, Sea of Okhotsk, and Sea of Japan” (Luchin et al., 2009). Symbols denote temperature conditions relative to 1988-2017: (see text for details). Note different scales for 0-300 and 300-1000 m depth intervals.

In the first half of the 1990s normal temperature conditions prevailed in summers in the water column of WBS. Only the upper 20-100 m layer had warm conditions in 1991-1993. The dichothermal layer was warm in 1995-2000, and the following several years were normal in terms of thermal state of this layer. The upper 50-100 m layer of the water column was cold at the same time. Warm and extremely warm conditions occurred roughly in the 0-600 m water column in 2004-2007. Cold conditions were observed in the dichothermal layer in 2008-2013. The warm intermediate layer was in warm and extremely warm states since 2006. The most recent years (2014-2017) reveal warm and extremely warm conditions throughout the whole 1000 m water column. This was likely due to warm water transport from the Pacific as the north-eastern Pacific Ocean experienced unusually warm conditions in 2014-2016.

During 2002-2012, the mean salinity of 0-50 m layer in summer-early fall in the WBS substantially decreased (Figure R16-6). Since 2013, there was a slight increase in the mean salinity of 0-50 m layer in summer, though the most recent measurements of 2017 are still below the level of 2002-2004. The variations in salinity of this layer in summer are largely determined by ice extent during previous winter. As more ice forms in the sea during winter, less saline is in the upper layer in summer (Khen et al., 2015).

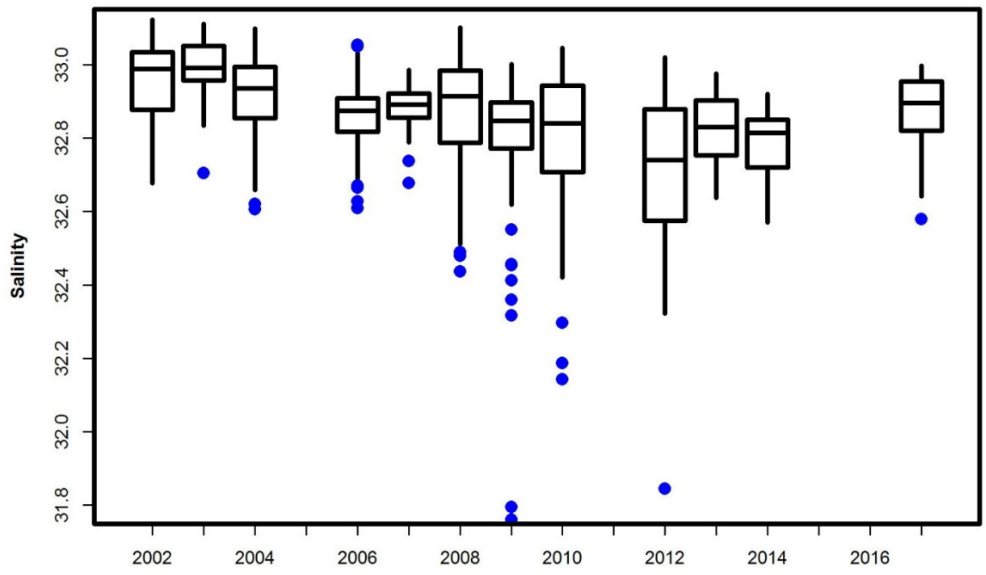

Figure R16-6. Box and whisker plot of mean salinity in the 0-50 m layer in September-October based on data of TINRO for 2002-2014 and 2017. Boxes represent quartiles, middle line is median, whiskers mark largest (smallest) value comparing to upper (lower) quartile plus (minus) 1.5 interquartile range; blue dots are outliers. Number of stations for 2002, 2003, 2004, 2006, 2007, 2008, 2009, 2010, 2012, 2013, 2014, and 2017 is 51, 45, 50, 91, 64, 68, 81, 133, 67, 90, 25, and 38, respectively. Data for September-October 2005, 2011, 2015 and 2016 are missing.

3.3. Sea surface temperature

Sea surface temperature data has been collected via remote sensing satellite technologies on a regular basis since 1979. Thus, it is a useful instrument in accessing the state of the abiotic part of the regional ecosystem. Together with other climatic information, often represented in form of atmospheric and oceanic indexes, it gives an idea of climatic fluctuations of the system.

To assess the changes in thermal state of the area, we used optimally interpolated monthly sea surface temperature (SST) data from NOAA's Earth System Research Laboratory (OISST v2). The data are available from https://www.esrl.noaa.gov/psd/data/gridded/data.noaa.oisst.v2.html. This dataset starts in January 1982 and has 1°×1° spatial resolution. The data were averaged for the whole Bering Sea (BS) and for the western Bering Sea area where the depth is greater than 200 m (WBS) as shown in Figure R16-7. SST values were weighted by the cosine of latitude. This averaging allows for comparison of the main temporal variability between the western Bering Sea and the sea as a whole. The data are represented as monthly SST anomalies for 1982-2017 (SSTA) relative to the mean values for every month for 1982-2012. We define winter months to be January, February and March, and summer months to be July, August and September. We define SSTA as "warm" in a particular month of a particular year if the value is greater than the multi-year mean for this month plus one standard deviation (SD). Similarly, where the SSTA value is lower than the multi-year mean for this month minus one SD, we define the record as "cold". All the values between the mean minus one SD and the mean plus one SD are defined as normal conditions.

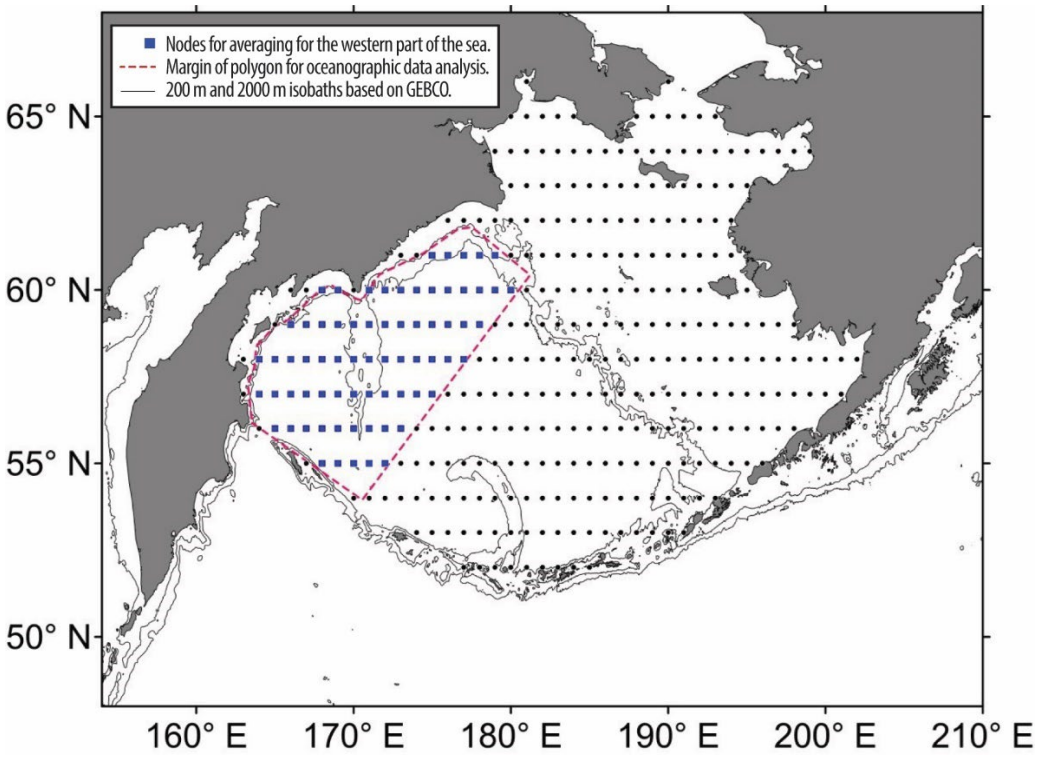

Figure R16-7. Distribution of grid nodes for SSTA analysis. Blue squares – nodes for averaging for the western part of the sea. Red dashed line represents the margin of polygon for oceanographic data analysis. Solid lines denote the 200 m and 2000 m isobaths based on GEBCO.

During the four past decades, both the BS and the WBS experienced substantial warming (Figure R16-8). In early 1980s, mean annual SST of the BS and WBS was about 4.2 °C and 4.1 °C, respectively. By the end of 2010s, the corresponding numbers were about 4.6 and 4.9 °C, respectively.

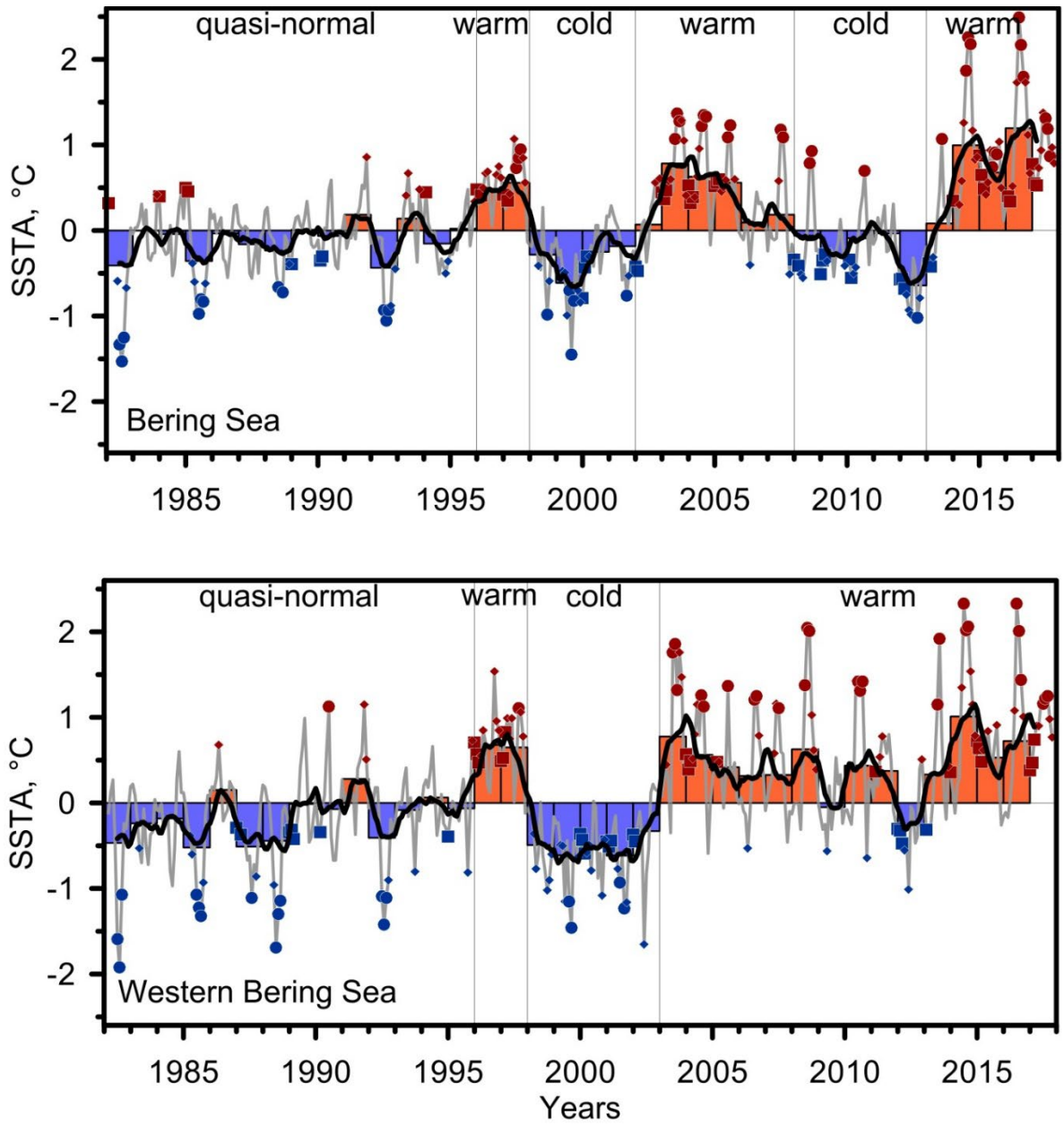

Figure R16-8. Time-series of Sea Surface Temperature Anomaly (SSTA) averaged over the whole Bering Sea (upper panel) and western Bering Sea (lower panel). Gray line denotes monthly SSTA relative to 1982-2012 multi-year mean. Black line is 13-month running average of monthly SSTA. Bars represent annual mean SSTA. Symbols mark warm (red) and cold (blue) months. Winter months (January-March) marked as larger squares, and summer months (July-September) marked as larger circles.

Several climatic states are evident in SSTA data in both the BS and WBS. Generally speaking, the surface temperature regime of the Bering Sea was quasi-normal from 1982-1995, warm in 1995-1998, cold in 1998-2002, warm in 2002-2008, and cold in 2008-2013. The last several years starting in 2013 show generally warm conditions both in the BS and WBS. It is worth noting that cold or warm regime does not imply all months within the time interval are cold or warm, respectively.

Despite general agreement between BS and WBS SSTA time-series, there had been several notable differences. For example, in the Bering Sea as a whole, several warm winter months occurred in the early to mid-80's (Figure R16-8a). This was not evident in the WBS, and winters there were mostly normal (Figure 16-8b). The timing of start and end of the thermal states slightly differ between those two areas also. For example, the cold regime from 1998 lasted one year longer in the WBS than in the BS. Moreover, the extremely cold winters of 2008 and 2009 which led to another shift in the eastern Bering Sea had little or no effect on surface temperature in the WBS. As a result, there was only a year-long deviation from the normal state into cold conditions in 2012 in the WBS area. More comprehensive analysis of SSTA dynamics in the BS and particularly the WBS may be found in (Baker et al., 2020).

When analyzing mean SST data, one should be aware that the values represent surface ocean conditions only. Moreover, this analysis describes combined effect of interactions between the sea and the atmosphere, and redistribution of heat by ocean currents.

3.4. Seasonal sea ice

We use sea ice data from NOAA's National Ice Center to describe interannual changes in mean winter ice cover. These data are available from www.natice.noaa.gov (1979-2009) and from http://www.nic.noaa.gov (2010-current) as daily shapefiles. This allowed us to calculate the area of ice cover for every day from 1999-2017 for the entire Bering Sea and for portion of the Bering Sea west of 180° E. The data were averaged for 10-day intervals and for every winter season (January-April). The western part of the Bering Sea is consistently less ice-covered in winter than the eastern shelf part. Sea ice covers only a narrow coastal band along the Koryak (Cape Olyutorsky to Cape Navarin) and Kamchatka coasts (Cape Navarin to south). Sea ice starts to grow in the Gulf of Anadyr in the middle of October. Outside of this gulf, sea ice forms in the embayments of the Koryak coast and inner part of the Korfa Gulf in mid-November. In December the rate of ice growth increases and peaks in February. Usually, ice cover stays at high level through the middle of April. The sea ice fields then disappear relatively quickly and the area is totally ice-free by the middle of June (Figure R16-9). In cold years (e.g. winter of 2011-2012) sea ice growth can last until the end of April. Contrarily, ice cover starts to disappear in February in warm years (e.g. winter of 2002-2003, Figure R16-9).

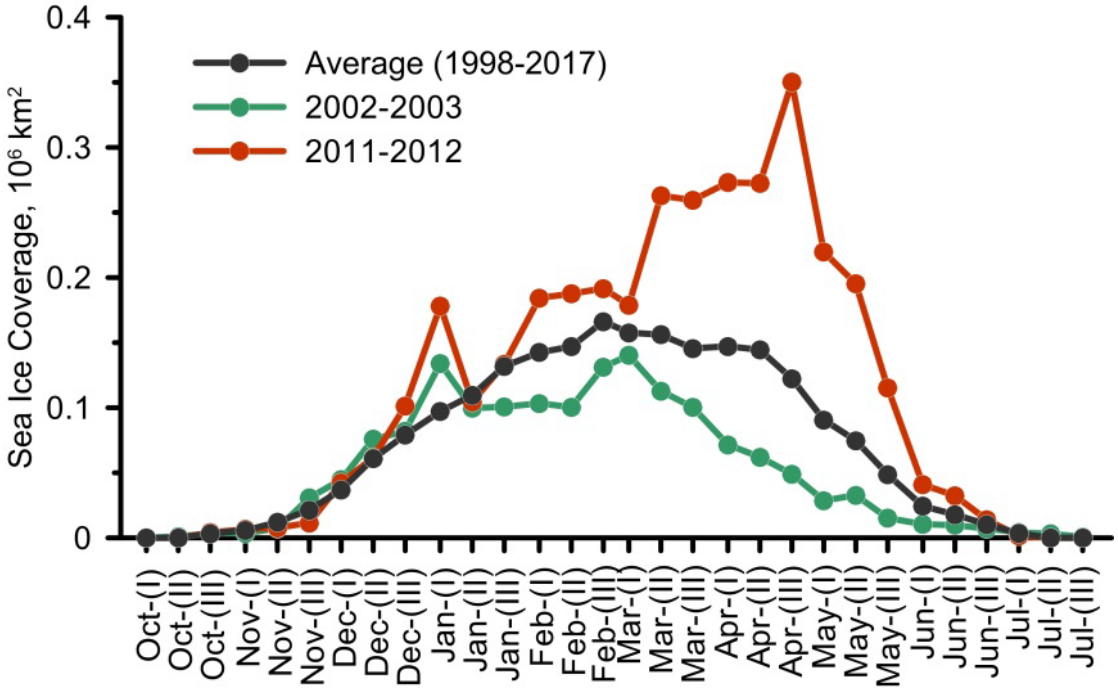

Figure R16-9. Seasonal changes in sea ice coverage across the western portion of the Bering Sea (west of 180° E). Red line represents high ice cover conditions of winter 2011-2012. Green line stands for winter of 2002-2003 with low ice cover. The black line is the average for 1998-2017.

The interannual variability of mean sea ice cover of the western portion of the Bering Sea generally mimics that for the total Bering Sea ice cover (Figure R16-10). The coefficient of correlation between those two time-series equals 0.6. Moreover, it is even higher (0.75) if the strong La Niña winter of 1999-2000 is excluded. Both areas experience general decrease of winter ice cover from 1999-2003 and 2012-2017.

The mean annual SST of the Bering Sea correlates well with maximum winter ice cover ($R = -0.73$). The mean annual SST of the Commander Basin also correlates with sea ice cover west to 180° ($R = -0.63$). At the same time, the mean annual SST of the Commander Basin is roughly independent of the maximum winter ice cover for the Bering Sea ($R = -0.16$).

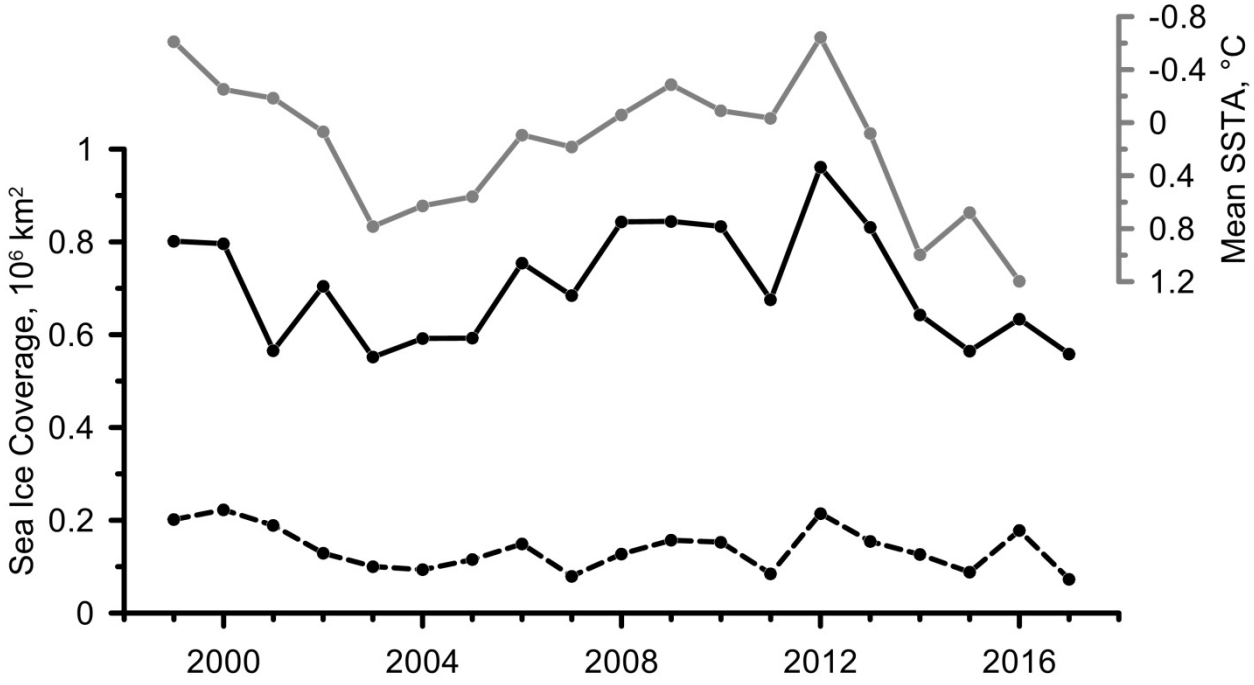

Figure R16-10. Interannual changes of sea ice cover (black lines, 10^6 km^2) in the Bering Sea (solid lines) and western portion of the Bering Sea. Grey line represents mean annual SSTA values (°C, note reversed axis) for the Bering Sea.

4. Chemical Oceanography

Contributor: K. Kivva.

The spatial distribution and temporal dynamics of the marine chemical constituents in the western Bering Sea depend both on physical processes (e.g. mixing and advection) and biological activity. Winter vertical mixing annually replenishes the nutrient capacity of the surface layer and brings subsurface waters with low concentration of dissolved oxygen (DO) and high concentration of nutrients to the surface layers. Nutrients are consumed in the euphotic layer (surface 0-40 m) by phytoplankton which produces new organic matter (OM) via photosynthesis. This occurs mostly in the spring-summer season. Different species of phytoplankton consume nutrients in different ratios. Dead OM (detritus) sinks from the surface layer to the deeper layers with simultaneous remineralization. Thus, surface waters contain smaller amount of nutrients in summer and autumn, at least until autumn mixing takes place. Conversely, deeper layers gain nutrients during summer. Phytoplankton produce DO in spring and summer in the euphotic layer. On the other hand, DO is consumed during OM remineralization in the deeper ocean. Ocean currents redistribute chemical species in all seasons, and mesoscale eddies may cause local upwelling or downwelling. Thus, characteristics of the chemical fields in any particular season depend on superposition of multiple factors including winter mixing intensity, spring-summer phytoplankton activity and composition, vertical fluxes during summer, and circulation features during the season.

4.1. Seasonal variability

During the past several decades as well as during 2009-2016, chemical oceanographic data were collected in the western Bering Sea on an irregular basis. Not much is yet known about seasonal dynamics of chemical constituents in the region. To put our research into broader context, it is necessary to discuss seasonal cycle of chemical constituents in the western Bering Sea. The existing dataset helps to shed light on this. Multiyear mean values of DO anomaly ($dO_2 = O_{2(observed)} - O_{2(saturation)}$), silicate and phosphate were calculated for 5-m bins with 10-day time steps between day of year 95 (beginning of April) and 295 (end of October). The data were selected from the deep western Bering Sea (see margin on Figure R16-7). As the data are not evenly distributed in terms of years and seasons and are quite limited, we performed smoothing in the time dimension. We used Gaussian weighting function ($w(d) = \exp(-d^2/2\tau^2)$), where d is time lag between time bin and date of observation, and τ is the width of the filter. Both the limit of d and the value of τ were set to be 15 days. For every time bin we considered observations done within 15 days prior to or after this date. This allowed us to fill most of the time bins and get a smoother picture. In order to avoid possible influence of anomalous years, the data were first processed year by year and mean values were calculated for the depths and seasons where data existed. Then individual values were averaged between years where several years with data were available. The resultant seasonal cycles of dO_2, silicate and phosphate within the upper 100 m of the water column are represented in Figure R16-11.

The water is under-saturated with DO by 20-30 μM which should be the reflection of winter OM decomposition. The maximum concentrations of the nutrients are observed in late March and April. Silicate and phosphate concentrations are about 50-52 and 1.9-2.0 μM, respectively. Unfortunately, we lack chemical information from May. However, existing satellite chlorophyll data suggest that main course of spring phytoplankton bloom (SPB) occurs in the western Bering Sea in May (Kivva and Kubriakov, 2021). Nutrients are partially consumed in the upper 20-30 m by the beginning of June. In June, the concentration of silicate and phosphate in this layer are 18-25 and 0.8-1.0 μM, respectively, and this layer is over-saturated with DO by 30-60 μM. Apparently, the SPB usually terminates in June, though some portion of primary production takes place later in summer season. The minimum nutrient concentrations are observed in the end of July. Concentrations of silicate and phosphate in the 0-10 m layer fall to 0.5-1.0 and about 0.1 μM, respectively. However, this result should be treated with caution as it is based on data mostly from areas within 300 km from the shore. There is some evidence that concentrations of nutrients are substantially higher in the central Bering Sea even in summer. DO production by phytoplankton becomes equal to DO consumption by OM remineralization in the upper 0-40 m layer in second half of August. The bulk of summer phytoplankton primary production is apparently done by this time of year. Interestingly, some amount of silicate and phosphate is still present in the euphotic layer within the region. Thus, primary production (PP) is not limited by those nutrients. It may be instead limited by nitrogen similar to the eastern Bering Sea shelf (Sambrotto et al., 1986, Lomas et al., 2012) or labile iron similar to the oceanic part of the Bering Sea (Leblanc et al., 2005). Some additional production occurs in the end of September-October, presumably after some autumn wind mixing brings more of those limiting elements to the upper ocean.

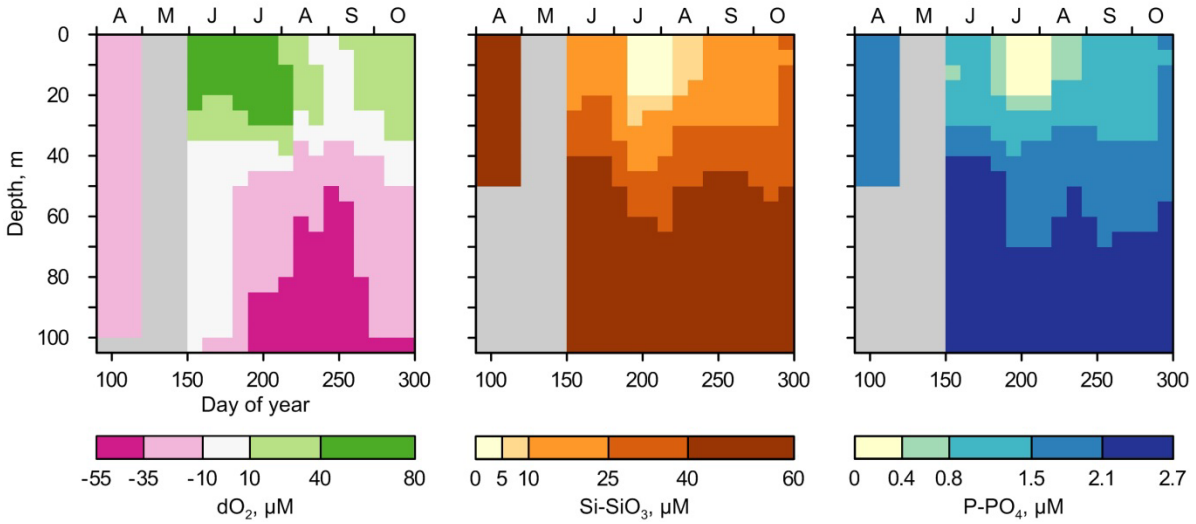

Figure R16-11. Multi-year (1970-2013) mean seasonal cycle of dissolved oxygen anomaly ($dO_2 = O_{2(observed)} - O_{2(saturation)}$), silicate and phosphate (µM) in the western Bering Sea. Grey color marks periods and depths with no reliable data.

One particularly important observation here is that chemical constituents in the western Bering Sea are quite variable during the year. Considering the quite limited data, it is difficult to choose a particular time of year for interannual dynamics analysis. It would be useful to assess the year-to-year changes in July but limited available data for this month prevents such analysis. The only opportunity for us to compare recent years in regard to chemical oceanographic dynamics is to use data from end of August to the beginning of October. Data from several cruises are available for this period and seasonal dynamics are quite moderate during this part of year.

4.2. Interannual variability

Chemical data are quite limited in the region of interest from 2009-2016. To the best of our knowledge, only four surveys of TINRO with chemical analyses are available. The distribution of measurements between the end of August and the beginning of October leaves only three years for comparison. So, we put those observations into the broader context of previous surveys of 2004 and 2008. To assess inter-annual changes in chemical setup, we calculate average dO_2, silicate and phosphate for depth intervals 0-30 m and 30-100 m for every available station. Then we performed a basic comparison between years without paying attention to the station distribution within the region as both in-shore and off-shore portions of the region were sampled with equal attention in analyzed years. This gives a general idea of interannual changes. However, it is difficult to determine the reasons for this variability as the distribution of chemical parameters in autumn is affected by many processes during winter, spring, and summer.

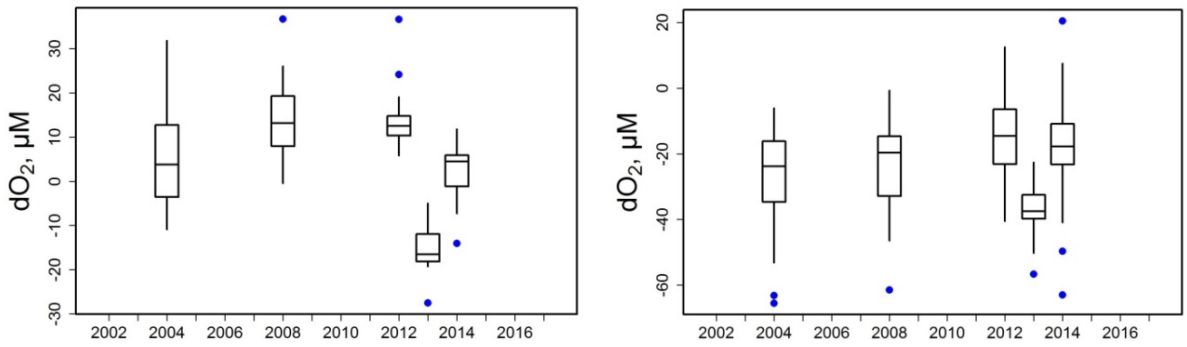

Figure R16-12. Statistics of mean 0-30 m (left panel) and 30-100 m (right panel) dissolved oxygen anomaly ($dO_2 = O_{2(observed)} - O_{2(saturation)}$, µM) in the western Bering Sea. Boxes represent quartiles, middle line is median, whiskers mark largest (smallest) value comparing to upper (lower) quartile plus (minus) 1.5 interquartile range; blue dots are outliers.

Interannual changes in dO_2 in the region show little difference between years from August-October. The only year which is significantly different from others is 2013 (Figure R16-12). During this year the whole water column was under-saturated with DO. This may be a reflection of high oxygen consumption by OM remineralization due to an unusually large phytoplankton bloom. This assumption is supported by relatively high mean concentration of both silicate and phosphate in the 30-100 m layer during 2013 (Figures R16-13 and R16-14). Preliminary results of analysis of remotely sensed chlorophyll-a also support this hypothesis (see next section).

Relatively low nutrient concentrations in the surface layer were observed in the WBS in September 2012 (Figures R16-13 and R16-14). As several processes alter nutrient distribution in autumn, it is difficult to determine the exact reason for this phenomenon. According to the temperature data (see section on 'Sea surface temperature', Figure R16-8), 2012 was extremely cold in the WBS. There were deep (down to approx. 300 m) negative temperature anomalies during 2012 as well (Figure R16-5). This means intensive and deep convective mixing in the area during winter of 2011-2012, which may lead to higher spring concentrations of all nutrients in the surface layer. Apparently, silicate and phosphorus do not limit PP in the region. However, limiting nutrients could be brought to the surface layer in higher concentrations in that year as well. This may allow higher consumption of silicate and phosphate in 2012 than in other years. At the same time this approach does not account for lateral advection which may play a role in redistribution of tracers in summer.

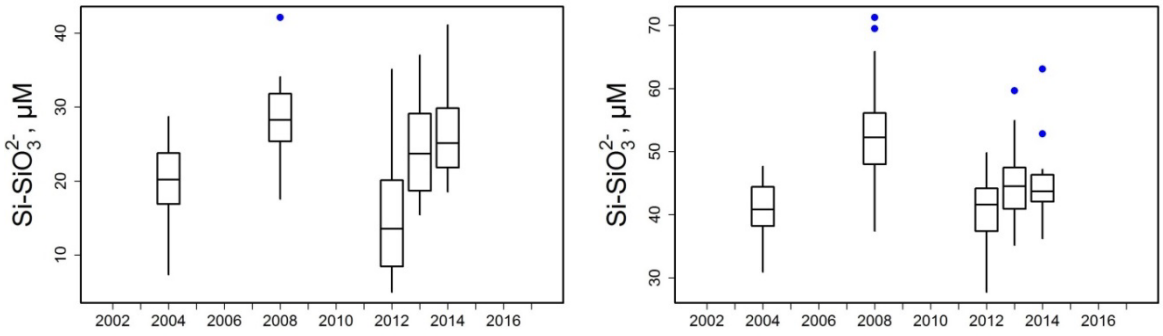

Figure R16-13. Statistics of mean silicate concentration (µM) in 0-30 m (left panel) and 30-100 m (right panel) layers in the western Bering Sea. Boxes represent quartiles, middle line is median, whiskers mark largest (smallest) value comparing to upper (lower) quartile plus (minus) 1.5 interquartile range; blue dots are outliers.

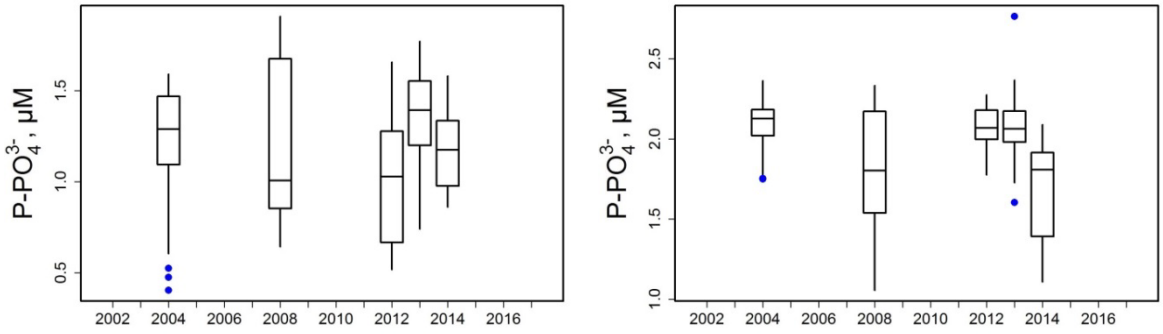

Figure R16-14. Statistics of mean phosphate concentration (µM) in 0-30 m (left panel) and 30-100 m (right panel) layers in the western Bering Sea. Boxes represent quartiles, middle line is median, whiskers mark largest (smallest) value comparing to upper (lower) quartile plus (minus) 1.5 interquartile range; blue dots are outliers.

5. Phytoplankton

Contributors: K.K. Kivva, A.A. Kubriakov

In situ sampling and observations of phytoplankton biomass, community composition, or pigment concentration are extremely sparse in the western Bering Sea region. To the best of our knowledge, no such sampling was performed from 2009-2016. Therefore, we assess the changes in chlorophyll-a concentration (Chl-a) using remotely-sensed data. We apply 8-day data from MODIS Aqua and analyze them from several aspects. First, we are interested in multi-year mean seasonal chlorophyll dynamics in the area and mean seasonal cycle of chlorophyll-a in three key areas of the western Bering Sea. Those are: the deep northern part of the Bering Sea near Cape Navarin, the western part of the sea near Kamchatka Strait, and in the oceanic domain of the sea (see Figure R16-16 for domain locations) Second, we focus on interannual variability in the three mentioned areas. The more comprehensive analysis of the data used in this section may be found in (Kivva and Kubriakov, 2021).

5.1. Mean areal chlorophyll-a distribution

According to the remotely sensed Chl-a data, the annual phytoplankton bloom starts in the WBS region in April and peaks in May (Figure R16-15). The higher concentrations of chlorophyll-a are observed annually in a wide stripe along the shelf break spreading to the deeper oceanic part of the sea. The bloom terminates mostly in June, but Chl-a slightly increases in the oceanic part of the sea during this time. Chl-a is generally low in July-September. A moderate increase in concentration takes place in October. This occurs apparently due to autumn wind mixing and may be called an autumn phytoplankton bloom.

In the most part of WBS region, the highest Chl-a values are observed in May. Chl-a peaks in June in oceanic part of the sea (Figure R16-16). A long and narrow strip of water along the west coast of the Bering Sea seems to experience the highest chlorophyll-a concentration in July-September. However, this may be an artifact of satellite data which is often erroneous in inshore areas. This may be due to chromophoric dissolved organic matter (CDOM) or particulate matter. In most of the area the lowest Chl-a concentrations are observed in February or March (Figure R16-16).

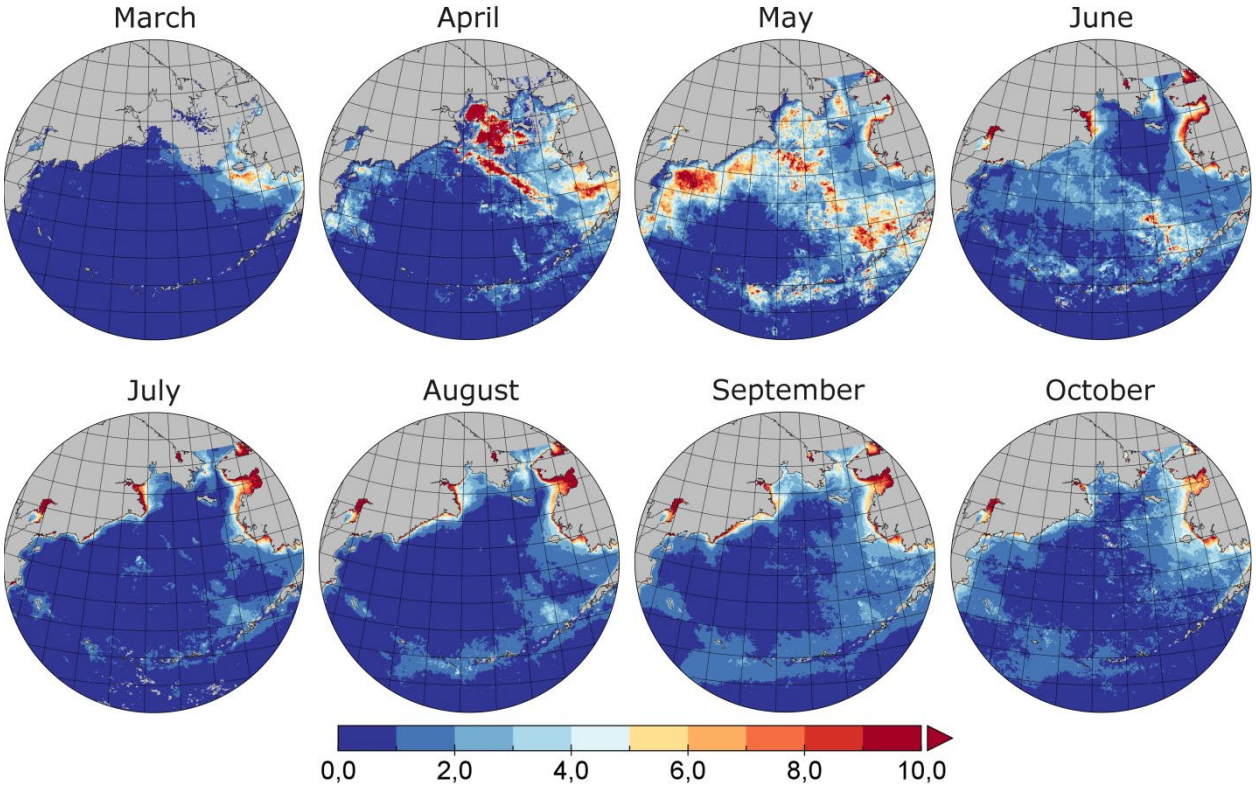

Figure R16-15. Monthly mean chlorophyll-a (mg m^{-3}) based on MODIS data from 2003-2017.

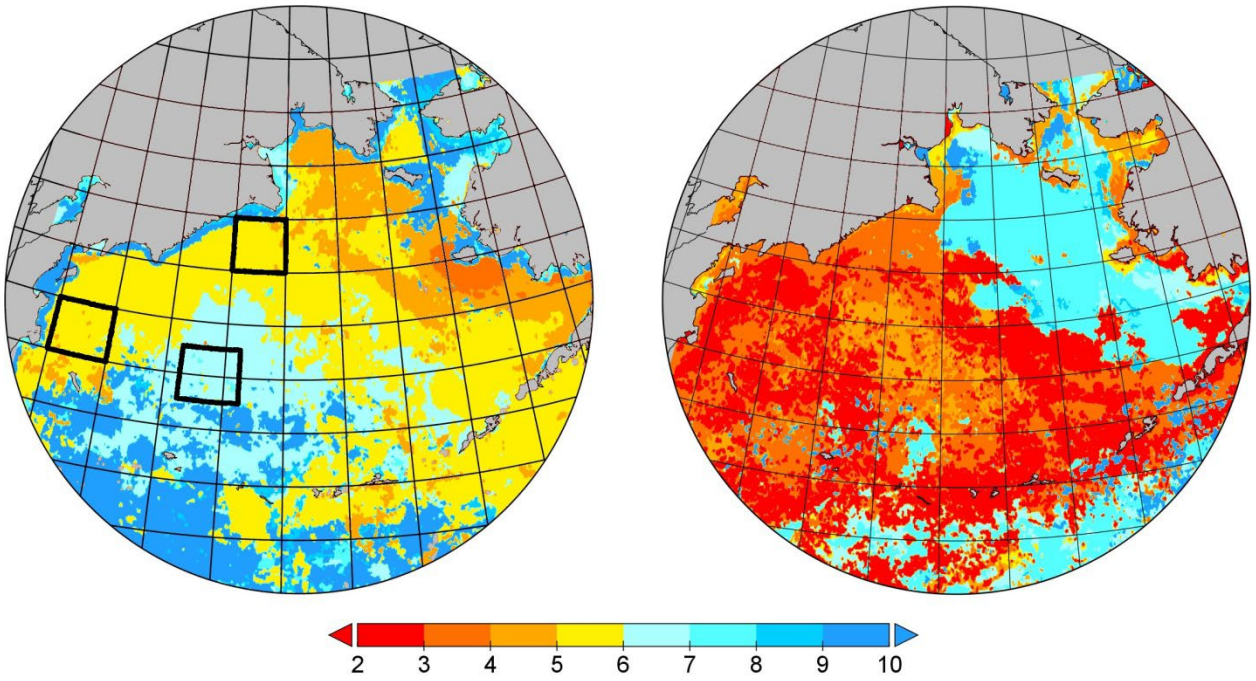

Figure R16-16. Multiyear mean month of maximum (left panel) and minimum (right panel) chlorophyll-a according to MODIS data for 2003-2017. Solid lines in the left panel mark regions of chlorophyll data averaging and analysis.

5.2. Seasonal dynamics of chlorophyll-a

Averaging of 8-day Chl-a values over areas of interest in the northern, western, and southern portion of the region allowed us to better describe seasonal dynamics of Chl-a. Western and northern portions of the WBS experience quite pronounced SPB. On the other hand, this feature is almost not visible in the central part of the sea (Figure R16-17) (Kivva and Kubriakov, 2021). SPB near Cape Navarin usually starts around middle of April. The highest between-years variability is observed there in the end of April and beginning of May. Phytoplankton reaches its maximum in the beginning of May in this area in some years, but it only starts to develop there in early May in other years. The SPB is usually over by the first half of June. However, relatively high mean Chl-a (5-7 mg m^{-3}) was observed up to late June in some years.

In the western portion of the WBS region, the SPB also usually starts in first half of April (Figure R16-17). However, the SPB may start there as early as middle of March. The SPB terminates in the western part of WBS before end of May. It is worth noting that the SPB there may last longer than in the northern portion of the region.

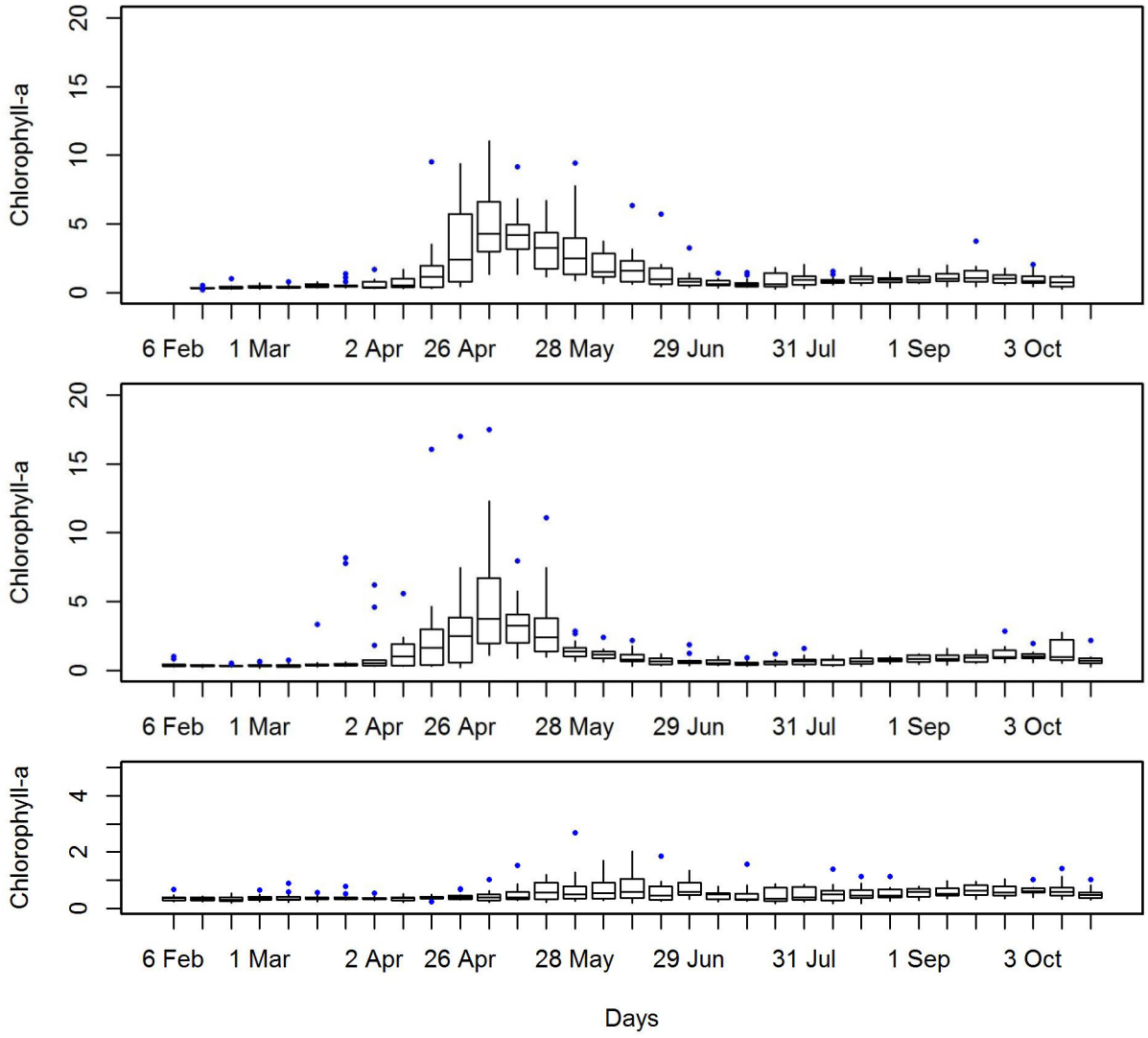

Figure R16-17. Interannual comparison of chlorophyll-a (mg m^{-3}) seasonal dynamics for three regions of the Bering Sea: northern area near Cape Navarin (upper), western area near Kamchatka Strait (middle), and area in oceanic domain (lower panel). The figure is based on MODIS data for 2003-2017, averaged over the regions for every 8-day interval. Boxes represent statistics between years. See location of regions in Figure R16-16. Boxes represent quartiles, middle line is median, whiskers mark largest (smallest) value comparing to upper (lower) quartile plus (minus) 1.5 interquartile range; blue dots are outliers. Note the different y-axis scale for the lower panel.

5.3. Interannual variability of phytoplankton bloom

The most pronounced differences between years occur in dates of start and end of the SPB. The date of the Chl-a maximum and integral of Chl-a (Chl-a values were multiplied by 8-days and summed over the SPB period, [mg day m^{-3}]) also show substantial variability. To assess these changes in the region, we focus on two areas, described above: near Cape Navarin, and near Kamchatka Strait, because the SPB is less pronounced in the oceanic part of the sea (Kivva and Kubriakov, 2021). We define dates of the SPB manually from MODIS data averaged over the areas of interest. The start date of the SPB was chosen as

the date before substantial increase of Chl-a. Consistently, the end date of the SPB was chosen to be the last date of relatively high Chl-a before it drops to summer levels. This approach has certain limitations. For instance, it is not always clear when the SPB ends. However, it gives a general idea of interannual SPB variability.

Relatively early SPBs occurred in 2004-2006, 2009, and 2013-2015 in the northern part of WBS region (area near Cape Navarin). Conversely, relatively late SPBs occurred there in 2008, 2010, and 2012 (Figure R16-18). Relatively high values of integral Chl-a over the SPB period were observed in this northern portion of WBS in 2005, 2006, 2009, 2012, 2014, and 2016. This parameter qualitatively reflects the strength of the bloom. Total amount of primary production during the bloom should follow this pattern. Overall, relatively early and relatively strong blooms were observed in this area in 2005, 2006, 2009, and 2014. Late blooms are usually less pronounced than early blooms in this northern area. There was a consistent transition from early blooms to later blooms in this area in 2013-2017.

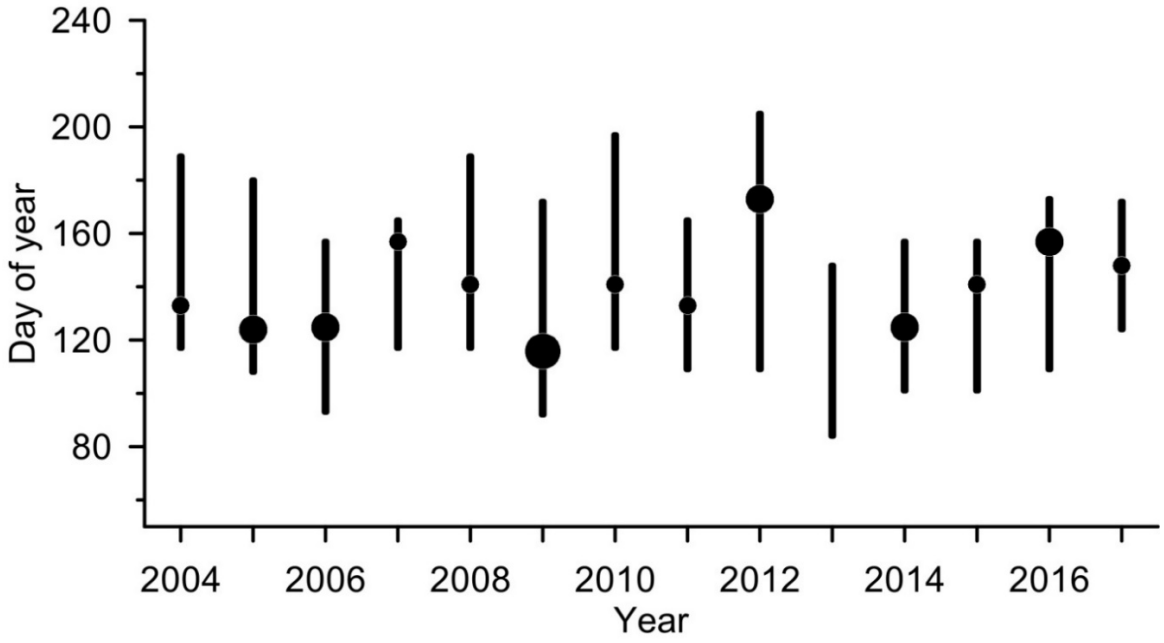

Figure R16-18. Interannual comparison of dates of spring phytoplankton bloom, and dates of maximum Chl-a in the northern portion of the western Bering Sea region near Cape Navarin (see Figure R16-16 for location of the region). Vertical lines denote dates of SPB, and circles mark the date of maximum Chl-a. The size of the symbol represents the integral of Chl-a during the SPB period (smallest circles – less than 200, median circles– between 200 and 300, and largest circles– greater than 300 mg day m^{-3}).

Overall the SPB dynamics are quite different in the western portion of the WBS region near Kamchatka Strait. Relatively early blooms occurred there in 2005, 2009, 2010, 2013, 2015-2017 (Figure R16-19). Relatively late blooms took place there in 2004, 2006-2008, 2011, and 2012. Earlier blooms are usually stronger in this area than late blooms. This result is consistent with analysis for the northern portion of the region. However, SPBs tend to start and end earlier in this area since roughly 2012.

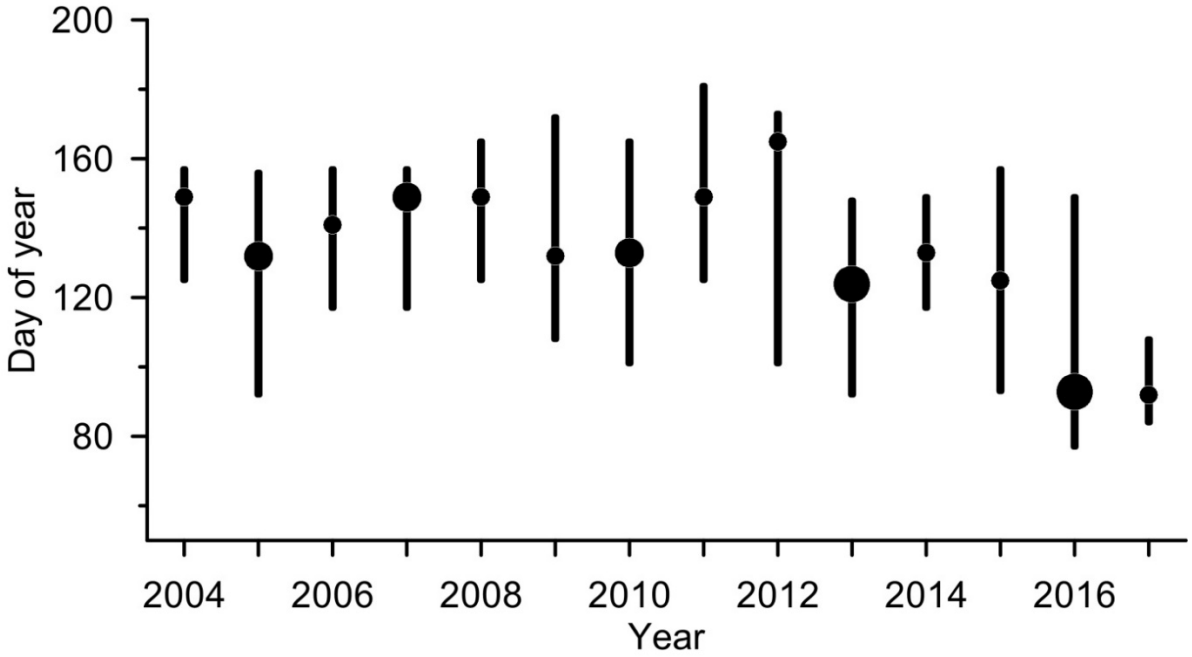

Figure R16-19. Interannual comparison of dates of spring phytoplankton bloom, and dates of maximum Chl-a in the western portion of the western Bering Sea near Kamchatka Strait (see Figure R16-16 for location of the region). Vertical lines denote dates of SPB, and symbols mark the date of maximum Chl-a. The size of the symbol represents the integral of Chl-a during the SPB period (smallest symbols – less than 200, median symbols – between 200 and 300, and largest symbols – greater than 300 mg day m^{-3}).

6. Meso-zooplankton

Contributors: M.A. Shebanova, N.A. Kuznetsova, K.K. Kivva.

Most of the fisheries research surveys of TINRO conducted during the past few decades in the western Bering Sea have included studies of zooplankton biomass distribution and community structure. Substantial amounts of data have been received during summer-autumn (June-October) surveys since 1986 on almost annual basis. Here we describe the main meso-zooplankton community structure changes in the deep portion of the western Bering Sea based on regions by Shuntov (1988) and Volvenko (2003). We analyzed data from their regions 7 and 8 which together are roughly identical to the deep western Bering Sea region used in other sections of this chapter (see Figure R16-7).

The same methods were used for zooplankton collection, identification and analysis every year since 1986. The methods are described in previous publications (Volkov, 1996; 2008; Borisov et al., 2004; Volvenko, 2021). Briefly, zooplankton has been collected with a Juday zooplankton net (mouth area 0.1 m^2, mesh size 0.168 mm) in 0-200 m layer. Vertical speed of the net was kept between 0.7-1.0 m s^{-1}. Samples have been divided into three fractions with three sieves (mesh size 0.5, 1.2 and 3.2 mm). Hereinafter the fractions are called small (body length between 0.5-1.2 mm), medium (1.2-3.2 mm) and large (>3.2 mm) zooplankton – SZ, MZ, and LZ, respectively. Abundance of SZ and MZ has been determined in a portion of the sample by a Bogorov counting camera. Abundance of LZ has been determined in total. Part of the zooplankton community avoids being caught by the net, so the following empirical coefficients have been used for correction of the results: 1.5 for SZ, 2.0 for MZ,

2.0, 5.0, and 10.0 for *Euphausia*, Mysidae and Chaetognatha with length <10, 10-20, and >20 mm respectively, 1.5, 3.0, and 5.0 for Hyperiidae with length <5, 5-10, and >10 mm respectively, 2 and 3 for Copepoda with length <5 and >5 respectively. Polychaeta, Medusae, Pteropoda and other slow-moving zooplankton were assumed to be unable to avoid the net (Volkov, 2008). Generalized results on zooplankton community biomass and composition in the western Bering Sea are present in Figures R16-20 and R16-21.

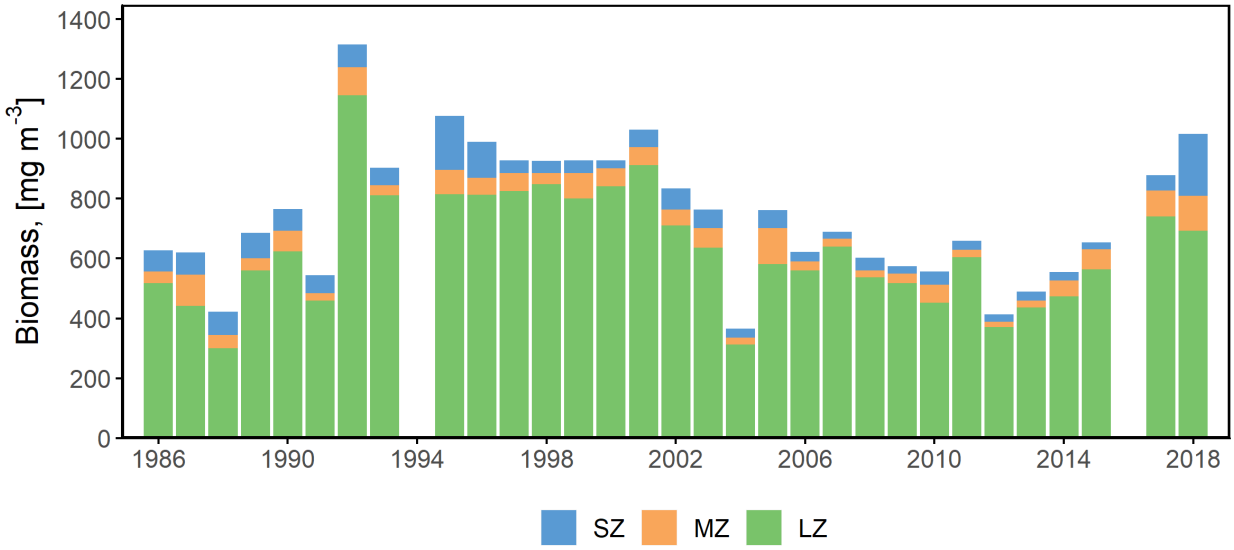

Figure R16-20. Interannual variability of zooplankton biomass by fraction (SZ – small, <1.2 mm, MZ – medium, 1.2-3.2 mm, and LZ – large zooplankton, >3.2 mm) in the 0-200 m layer of the WBS. In different years the samples were collected in June-October.

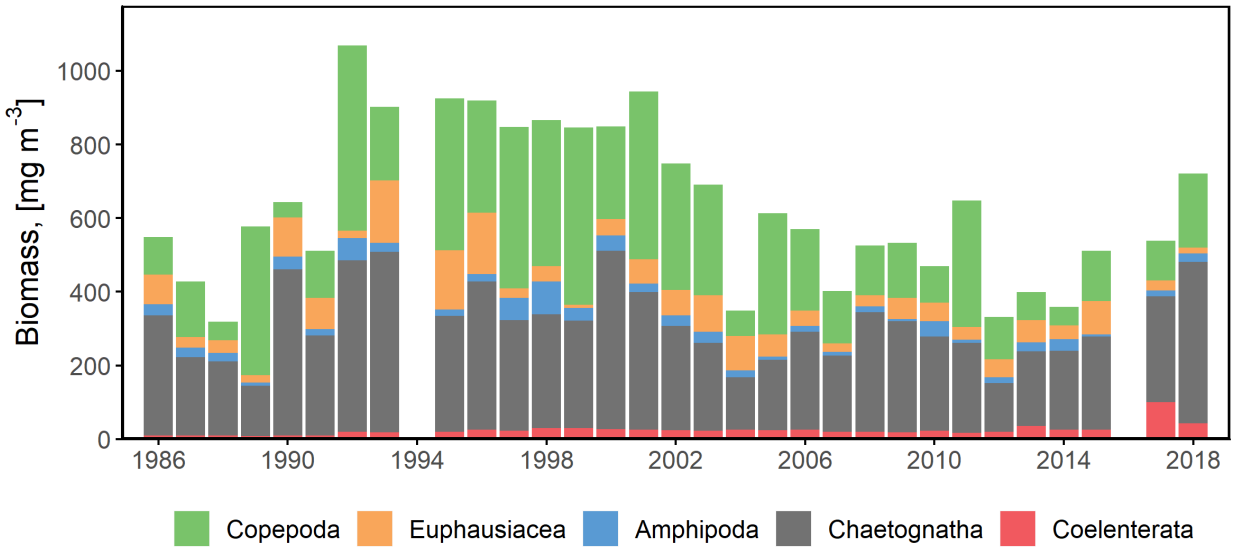

Figure R16-21. Interannual variability of biomass of main zooplankton taxa in the 0-200 m layer of the WBS. The samples were collected in June-October.

The first five most dominant species were same in all study years in the Bering Sea. Every year the same 10 species contribute about 94 % of total zooplankton biomass. The small (SZ) and medium zooplankton (MZ) are usually dominated by *Pseudocalanus* spp., *Oithona similis* and juveniles of *Themisto pacifica*. The dominant species of large zooplankton fraction (LZ) usually include *Sagitta elegans*, *Aglantha digitale*, *Neocalanus plumchrus*, *Eucalanus bungii*, and *T. pacifica*.

In 2009-2011 the biomass of zooplankton was virtually stable with values about 600-800 mg m^{-3}. LZ contributed between 81-92 % of total zooplankton biomass. The dominant taxa were Euphausia, Copepoda, and Chaetognatha. In 2012 the zooplankton biomass had decreased to about 400 mg m^{-3}. This was probably a reflection of zooplankton community change. Despite the biomass of other taxa remaining the same, biomass of Copepoda and Chaetognatha declined roughly by half. The waters of the Bering Sea started to experience warming in 2013. At the same time an increase of relative abundance of Chaetognatha and Hyperiidae (Amphipoda) was observed. The mean zooplankton biomass in 2013 was observed to be 382-394 mg m^{-3}. In 2014, as well as before, LZ contributed the largest portion of zooplankton biomass (81.5-94.3 %). The mean biomass of this LZ fraction in 2014 was 818 mg m^{-3}. At the same time the ratio of this fraction was relatively low (about 27.5 %) in the coastal area between Cape Olyutorsky and Cape Navarin (Koryak Coast). However, the deeper region south-east to Cape Navarin experienced the highest concentration of LZ – 1031 mg m^{-3}. In 2014 LZ was dominated by Euphausia (25.6-54.1 % of LZ biomass), Chaetognatha (26.4-49.3 %), and Copepoda (15.0-21.8 %). On the other hand, Hyperiidae experienced low biomass due to a decline of *Themisto libellula*.

Zooplankton biomass varied between 594-772 mg m^{-3} in the deep WBS in 2017, and LZ contributed 74-84 % of total zooplankton biomass. MZ and SZ contributed 5-11 and 11-15 % of total zooplankton biomass respectively. The most abundant groups in the deep WBS region were Chaetognatha and Copepoda. *S. elegans* was dominant with biomass between 230-340 mg m^{-3}. However, in the south-western part of the region other dominant species included *N. plumchrus* and *E. bungii* (105-110 mg m^{-3}). At the same time, *A. digitale* occupied the second place by biomass after Chaetognatha in northern part of the region, and other dominant species included Hyperiida *T. pacifica* and the small copepod *O. similis*.

In 2018, the biomass of zooplankton was generally higher than in 2017 (439.5-1767 mg m^{-3}). The proportion of different fractions was roughly similar to 2017. Six groups contributed the most to the biomass, including Chaetognatha (*S. elegans*), Copepoda (*O. similis, N. plumchrus, E. bungii, Metridia pacifica, N. cristatus*), Hyperiidae (*T. pacifica*), Hydromedusae (*A. digitale*), Syphonophorae (Diphyes sp.), and Euphausia (*Thysanoessa longipes*). The Chaetognatha *S. elegans* dominated there during the summer survey (biomass between 363-430 mg m^{-3}) contributing about half of LZ (36-42 %). The other dominating taxa included Copepoda (161-250 mg m^{-3}, about 22-35 %) and medusa (about 50 mg m^{-3}, 4-10 %).

The comparison of mean zooplankton biomass estimates and its components for 2009-2015 reveals slight variations of biomass of some groups and fractions (note there is no data for 2016). Considerable changes were observed since 2017 almost exclusively in SZ fraction. The copepod *O. similis* was responsible for doubling of SZ biomass from 2017 to 2018. Warm conditions of 2018 may be a reason for the success of the autumn generation of this species.

Despite the described boreal and wide-spread species of zooplankton contributing the largest part of zooplankton biomass in investigated regions, species of subtropical or transitional waters were also observed in all study years. In LZ these were south-boreal copepod species *Calanus pacificus* and *Candacia bipinnata*. In MZ and SZ fractions the characteristic examples are *Paracalanus parvus* and *Mesocalanus tenuicornis*. Relative abundance of warm-water species in zooplankton of northern seas of North Pacific depends on features and intensity of climatic and oceanographic processes (Shuntov, 2001). Another example of unusual species appearance is episodic deep species transport to epipelagic layer. For instance, warm conditions in the upper 500 meters of the water column in 2017 (temperature anomaly in cold intermediate layer of about 1.5-2.0 °C) resulted in enhancement of vertical water exchange in the region. This led to more pronounced appearance of typically deep water species of zooplankton to the epipelagic layer. Examples include the copepods *Pleuromamma scutullata*, *C. columbiae* and *Heterorhabdus tanneri*.

7. Fishes and Invertebrates

Contributors: A.A. Somov, K.K. Kivva.

7.1. Fish community structure and dynamics

The epipelagic zone of the deep basins of the western Bering Sea is an important transit zone for numerous commercially valuable species (Shuntov, 2016). Pacific salmon and squid perform annual migrations there in the summer-fall season. Other species such as herring (*Clupea pallasii*) and walleye pollock (*Theragra chalcogramma*) migrate there but are only abundant in some years (Shuntov et al., 1993, Shuntov, 2016). TINRO conducts regular research fisheries surveys in this area. Seventeen such surveys were performed there in 2003-2015 with 1417 scientific trawling operations. The same ships with the same trawling equipment (squared mesh midwater rope trawl, model RT 80/396 with fine-meshed (10mm) inset in the cod end) were used for every haul. The vessel speed during trawl operations was kept between 4 to 5 knots (mean value – 4.6). The mean trawling area was 0.333 km^2 h^{-1}, calculated using the horizontal trawl opening (mean – 40 m). The trawl headrope was held at the surface.

The total biomass of trawl fauna varied between 490-3400 kg km^{-2} in 2003-2015 with mean value of 1300 kg km^2. The nekton biomass was in range 450-1800 kg km^{-2} (mean 825 kg km^{-2}). The biomass of gelatinous plankton in the total trawl catch was 10-2660 kg km^2 and its ratio to total catch was 2-78 % with mean value of 26 %.

As in many other regions of the North Pacific, Pacific salmon dominate the fish community (ichtyocoenose) of the epipelagic zone during their migration in summer and fall in the WBS (Shuntov and Temnykh, 2011). However, the WBS is dominated by chum salmon (*Oncorhynchus keta*), unlike the Sea of Okhotsk and Kuroshio-Oyashio Region which are mostly dominated by pink salmon (*O. gorbuscha*) in summer and fall seasons (Ivanov, 1998; Temnykh et al., 2003; Khoruzhiy, 2011). This is due to the fact that numerous salmon populations, which winter in the ocean more than 1 year (chum, sockeye, chinook), migrate to the WBS for feeding. These populations are from various coasts (Russia, Japan, North America) (Bugaev, 2007a, 2007b; Bugaev et al., 2007; Urawa et al., 2009; Shuntov and Temnykh, 2011). Key species and their multi-year mean biomass are summarized in Table R16-1.

Table R16-1. Relative abundance of key species in the pelagic zone of the deep part of the western Bering Sea

Name	Group	Biomass kg km^{-2}	SD+	SD-	SE+	SE-
Oncorhynchus keta	Anadromous	476.0	120.0	41.1	10.2	8.6
Boreoteuthis borealis	Squid	83.3	92.6	14.5	10.6	6.3
Oncorhynchus nerka	Anadromous	74.7	38.2	12.3	3.1	2.6
Oncorhynchus gorbuscha	Anadromous	45.9	177.5	45.9	12.2	9.9
Oncorhynchus tschawytscha	Anadromous	21.9	1.6	0.7	0.2	0.2
Clupea pallasii	Pelagic	15.5	54.0	8.9	9.4	3.9
Gonatus kamtschaticus	Squid	10.9	4.4	2.0	0.3	0.6
Cololabis saira	Southern migrant	9.3	95.7	9.0	10.2	3.3
Salvelinus malma	Anadromous	8.8	7.7	2.0	1.0	0.8
Leuroglossus schmidti	Mesopelagic	6.4	12.8	3.8	2.1	1.1
Pleurogrammus	Pelagic	6.2	15.5	2.7	1.0	0.8
Brama japonica	Southern migrant	4.8	1.1	0.5	0.5	0.3
Oncorhynchus kisutch	Anadromous	4.4	1.5	0.9	0.2	0.2
Aptocyclus ventricosus	Pelagic	3.2	3.2	2.9	0.3	0.7
Other species		22.1	40.2	32.4	2.7	9.3

Note: SD – standard deviation; SE – standard error; positive and negative values of SD and SE differ because means were calculated for log-transformed values.

7.2. Seasonal variability of epipelagic fish community composition

TINRO Fisheries research surveys were conducted in the western Bering Sea in June-October in different years. Available information allows us to nominally divide this period into three parts: early summer (1 June - 20 July), late summer (21 July - 20 September), and fall (21 September - 30 October) (Somov, 2017).

In the early summer, the mean total nekton biomass is 478 kg/km^2. During this period, the large fraction of pre-anadromous mature salmon, especially chum and pink salmon, is characteristic for the epipelagic fish community in the deep western Bering Sea (Figure R19-20). Pink salmon dominate in the community only during the peak of their migration - late June - early July. However, pink and chum salmon are differently spaced in the WBS. Pink salmon are mostly condensed in the western portion of the region as their main spawning area is located in the Karaginsky Bay. They migrate there through the Near Strait and cross the southern part of the sea. Chum salmon are concentrated mostly in the north-eastern part of the region where they migrate to the Gulf of Anadyr and Koryak coast. At the same time, mature sockeye salmon migrate mostly to the adjacent waters of the Pacific Ocean, south of the Commander Islands. Immature feeding salmon are not very abundant in the epipelagic zone of the WBS in early summer as they only have begun to migrate there.

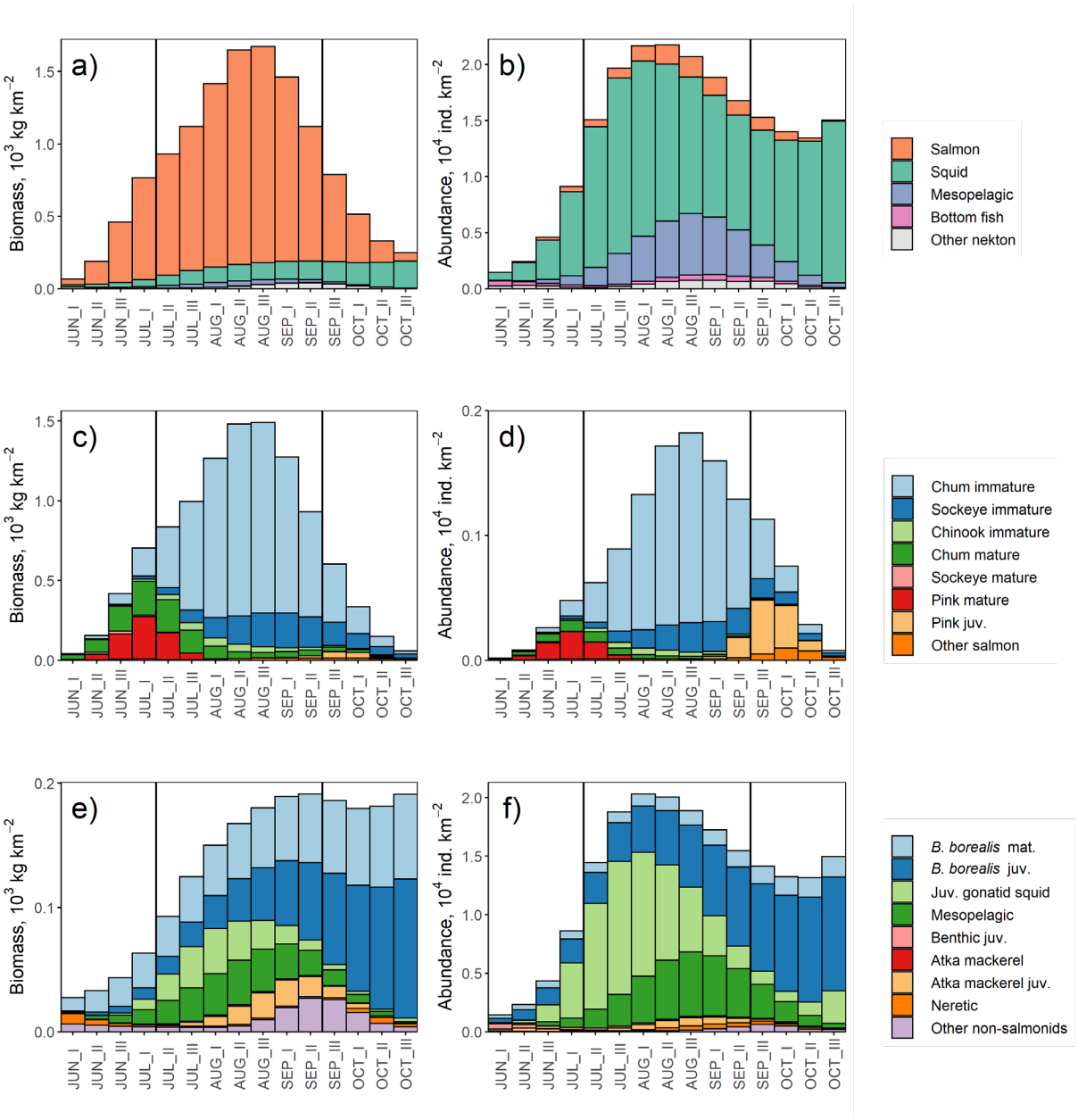

Figure R16-22. Seasonal variability of nekton community structure in the upper epipelagic layer of the WBS. Left panels (a, c, e) – biomass, 10^3 kg km^{-2}, right panels (b, d, f) – abundance, 10^4 ind. km^{-2}. Top row (a, b) – all species with rough division into groups; middle row (c, d) – only salmon; bottom row (e, f) – all species except salmon. Vertical lines denote margins of early summer, late summer, and fall. The plots are based on TINRO fishery surveys data from 2003-2015. Note different y-axis scales in different panels.

Pacific herring are a neretic (shelf) species, but it still may contribute a significant fraction to the fish community of the deep WBS. Pacific herring migrate from wintering areas in Karaginsky Gulf and Olyutorsky Gulf to feed near Cape Navarin and as far as Gulf of Anadyr in spring and summer. They spread to the deep Bering Sea when their population is large (Naumenko, 2010; Loboda and Zhigalin, 2017).

Recruit squids are usually abundant in the WBS in early summer. The most abundant squid species in the WBS are *Boreoteuthis borealis* and *Gonatus kamtschaticus*. Both mature and immature individuals of those species are transported from the Pacific Ocean to the Bering Sea by currents. However, the abundance of mature individuals of *B. borealis* and *G. kamtschaticus* is 2-3 and 10-15 times less than abundance of their juveniles.

Immature individuals of bottom fish are quite abundant (5'000-10'000 ind. km^{-2}) at the very beginning of the early summer period in the study area, although their abundance decreases significantly by the end of this period. Only Atka mackerel (*Pleurogrammus monopterygius*) are abundant during whole summer-fall period.

Mesopelagic fishes perform diurnal vertical migrations to the epipelagic zone at night. They are concentrated in the south-eastern part of the WBS. Considering the small size and sedentary life style of most mesopelagic species, one may assume their distribution with currents similar to squid (Watanabe et al., 2006). However, according to the distribution patterns, mesopelagic fishes are more abundant in the deep Bering Sea outside of the western region.

In the late summer total nekton biomass increases nearly 3 times compared to the early summer and reaches 1400 kg/km^2. Immature salmon become the most abundant group of species and spread across the whole area. Their migration to the region is differentiated in time by age. Larger and older individuals migrate there first, and smaller individuals follow them (Zavolokina and Zavolokin, 2007; Shuntov and Temnykh, 2011). This is true for pink, chum, and sockeye salmon. Immature chum salmon dominate the fish community in the late summer. They may contribute up to 60-70 % of total nekton biomass. Mature salmon mostly complete their migrations before the late summer. Only mature chum salmon are relatively abundant in the epipelagic zone of the WBS during summer-fall period as it has both summer and autumn forms. All Pacific salmon together may contribute up to 80 % of total nekton biomass in late summer.

Total nekton biomass drops to early summer values (about 480 kg km^{-2}) by the beginning of fall period. Squids start to play more important role in the community at this stage. They contribute up to 50-60 % of nekton biomass by the middle of fall season.

Immature feeding salmon are still present in the WBS region in fall. However, they start migrations towards the Pacific Ocean for overwintering at this time. Therefore, their contribution to the nekton community drops from 50-60 % in early fall to 10-20 % in late fall. Juvenile salmon start to appear in the region in late summer. They are distributed across the whole region by fall. Pink salmon forms the most significant fraction. They contribute about 16 % of total nekton biomass in fall in Commander Basin. Other Pacific salmon recruits are more than 10 times less abundant in the area.

B. borealis usually becomes the most abundant species in the WBS epipelagic zone in the middle of fall due to the migration of salmon. Moreover, the vertical distribution of squids is wider than the epipelagic zone and only a portion of squid migrate to the epipelagic layer, resulting in an underestimate of squid in these surveys. *B. borealis* and immature individuals of other squids are evenly distributed in the WBS in fall. Abundance of immature squid in the epipelagic layer decreases by the end of fall. This may be due to predation (Radchenko, 1992) or ontogenetic migration to deeper layers (Roper and Young, 1975; Bower and Tagaki, 2004; Katugin and Zuev, 2007).

Southern migrants may be found in the south-eastern part of the WBS during favorable oceanographic conditions. They include Pacific pomfret – *Brama japonica*, Pacific saury – *Cololabis saira*, Pacific spiny dogfish – *Squalus suckleyi*, Japanese anchovy – *Engraulis*

japonicus, Japanese flying squid – *Todarodes pacificus*, and boreal clubhook squid – *Onychoteuthis borealijaponica* (Glebov et al., 2004; 2010a, 2010b; Savinykh, 1994; Bajtalyuk and Davydova, 2002). Pacific pomfret and Pacific saury are the only species amongst those mentioned above which make up a significant fraction of the nekton biomass. In the 2018 survey in the WBS large schools of Japanese sardine were identified – it was the first record of this species in the WBS in the last 30 years.

Summary of seasonal changes in epipelagic fish community is given in Table R16-2.

Table R16-2. Seasonal changes in relative abundance of key species in epipelagic zone of the deep western Bering Sea in summer and fall

Species	Biomass, kg km^{-2}			SD			SE		
	ES	LS	F	ES	LS	F	ES	LS	F
Chum	240.4	1016.9	170.7	+184.5 −67.8	+577.4 −251.2	+213.9 −69.3	+20.8 −16.5	+128.2 −91.4	+9.9 −8.9
Sockeye	17.8	125.4	80.7	+15.9 −4.9	+160.2 −43	+96.6 −28.2	+1.6 −1.2	+24.3 −14.5	+4.7 −4.2
Pink	104.0	10.0	23.7	+162 −41.9	+15.3 −5	+104.5 −11.4	+8.9 −7.7	+3 −2.1	+3 −2.4
Chinook	8.1	51.5	6.0	+22.8 −4.6	+76.5 −26.9	+4.5 −1.5	+2.3 −1.7	+18 −11.8	+0.7 −0.5
Coho	0.3	7.7	5.2	+0 −0	+1.3 −0.8	+2.8 −1	+0 −0	+0.5 −0.4	+0.3 −0.3
Dolly Varden	19.8	6.2	0.0	+42.2 −11.6	+9 −2.5	+0 −0	+4.2 −2.7	+2.6 −1.4	+0 −0
All salmon	**390.4**	**1217.6**	**286.3**	**+250.6 −80.9**	**+604.3 −256.3**	**+256.9 −75.7**	**+23.2 −18.5**	**+131.8 −93.3**	**+11.3 −10.1**
Boreopacific gonate squid	26.2	84.6	139.1	+176.5 −7.6	+116.7 −22.3	+272.1 −28.7	+17.4 −5.6	+34.3 −13.4	+48.4 −17
Shortarm gonate squid	3.1	24.4	5.4	+5.7 −1	+131.2 −10.3	+6.9 −1.7	+0.5 −0.3	+11.1 −5	+1.2 −0.8
Juveniles of gonatid squids	1.0	0.1	1.4	+3 −0.6	+0.1 −0	+2.1 −0.4	+0.6 −0.3	+0 −0	+0.3 −0.2
Other cephalopods	*1.8*	*1.9*	*1.8*	+0.5 −0.2	+0.4 −0.2	+0.5 −0.2	+0.2 −0.1	+0.1 −0.1	+0.1 −0.1
All cephalopods	**32.1**	**111.0**	**147.7**	**+176.6 −7.7**	**+175.6 −24.5**	**+272.2 −28.7**	**+17.5 −5.6**	**+36.1 −14.3**	**+48.4 −17.1**
Northern smoothtongue	7.4	7.5	4.1	+27.3 −2.6	+44.2 −2.3	+10.4 −1.5	+6.4 −1.8	+3.8 −1.3	+0.8 −0.5
Scaly paperbone	3.0	1.6	2.0	+3.1 −0.8	+0.4 −0.1	+3.5 −0.6	+0.7 −0.4	+0.1 −0	+0.3 −0.2
Northern lampfish	0.1	6.9	2.1	+0.9 −0	+48.1 −3.1	+15.4 −1.1	+0.3 −0	+4.8 −1.7	+1 −0.4
Other mesopelagic fishes	*0.1*	*0.1*	*0.1*	+0.2 −0	+0 −0	+0.2 −0	+0.1 −0	+0 −0	+0 −0
All mesopelagic fishes	**10.6**	**16.1**	**8.3**	**+27.5 −2.7**	**+65.4 −3.9**	**+18.9 −1.9**	**+6.5 −1.9**	**+6.1 −2.2**	**+1.3 −0.7**
All migrants	**0.0**	**16.5**	**11.7**	**+0 −0**	**+961.6 −13.9**	**+49.7 −5.8**	**+0 −0**	**+82.9 −5.2**	**+6.1 −3.1**
Pollock	1.9	27.6	1.4	+21.8 −5.1	+44.1 −5	+51.9 −3	+3.5 −2.3	+2.9 −1.8	+2.6 −1.4
Herring	35.4	3.8	7.1	+616.1 −35.5	+0.6 −0.2	+45 −4.3	+36.2 −18.4	+0.2 −0.1	+4.2 −2.2
Atka mackerel	0.2	14.0	4.5	+0.9 −0.1	+64.3 −6.5	+25.3 −2.3	+0.1 −0.1	+4.8 −2.3	+0.7 −0.5
Capelin	1.6	0.1	7.8	+0 −0	+0 −0	+265.4 −3.7	+0 −0	+0 −0	+73.2 −3.6
Demersal fishes	4.3	4.0	1.9	+3.2 −1.5	+2 −0.3	+10.4 −0.9	+2 −1.2	+0.5 −0.2	+1.5 −0.5
Other species	*1.7*	*11.9*	*2.1*	+0.2 −0.1	+0.8 −0.2	+6.5 −0.3	+0.1 −0	+0.2 −0.1	+0.2 −0.1
All nekton	**478.2**	**1422.7**	**478.8**	**+688.5 −88.8**	**+1151. −258**	**+467.5 −81.5**	**+46.5 −27**	**+159.9 −94.6**	**+88.9 −20.6**

Note: ES – early summer, LS – late summer, F – fall; data were log-transformed; upper values of SD and SE are positive values, lower values are negative values.

7.3. Interannual variability of epipelagic fish community composition

The years of 2003-2015 may be divided into two periods based on total abundance of epipelagic fauna. This parameter was relatively high in 2003-2009, and subsequently relatively low in 2010-2015. This was true for both nekton and gelatinous macrozooplankton (Figure R16-23). We note that macrozooplankton abundance experienced a more pronounced change than nekton.

Most of the species revealed a substantial increase of biomass in 2003-2009. The most obvious changes occurred in biomass of Pacific salmon, squid, mesopelagic fish, and recruits of bottom fish. The mean total biomass of nekton changed almost two-fold from 1080 kg km^{-2} in 2003-2009 to 530 kg km^{-2} in 2010-2015. The highest values of weighted mean nekton biomass were observed in 2003 and 2005 (1400 and 1800 kg km^{-2}). The lowest weighted mean nekton biomass (455 kg km^{-2}) was observed in 2010. At the same time, Atka mackerel, herring, and southern migrators biomass rose during the whole interval of 2003-2015 (Figure R16-24).

Jellyfish (macrozooplankton) biomass decreased more than six-fold between 2003-2009 and 2010-2015. The mean jellyfish biomass was 800 and 125 kg km^{-2} in 2003-2009 and 2010-2015, respectively. The highest values of jellyfish biomass were observed in 2004 and 2006 – 2660 and 1600 kg km^{-2}, respectively. The lowest biomass of jellyfish was observed in 2010 and 2011 (35 and 10 kg km^{-2}, respectively).

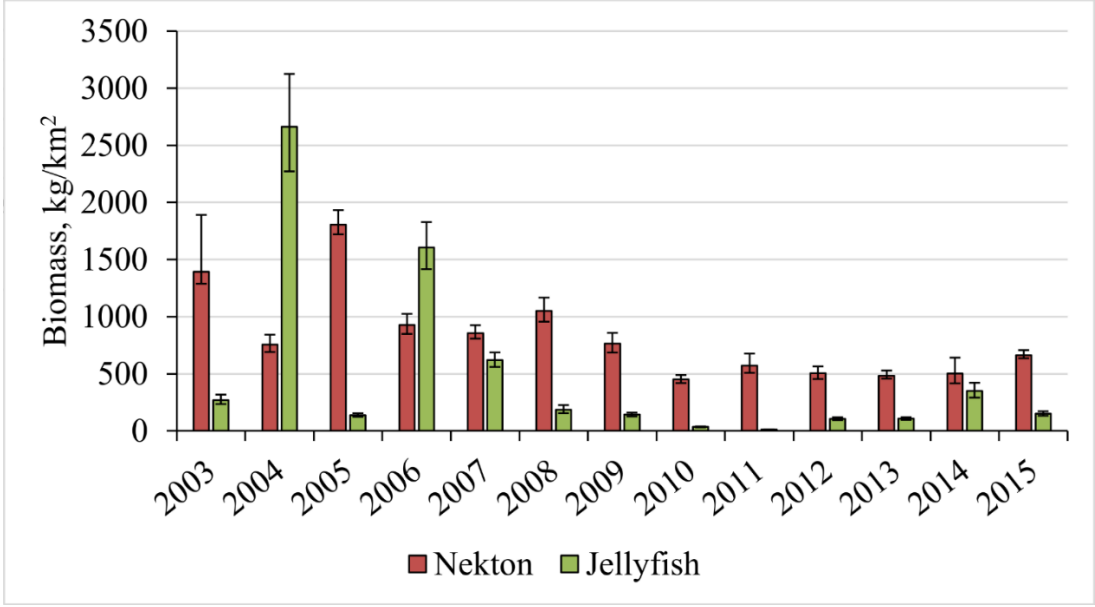

Figure R16-23. Interannual dynamics of mean nekton and macrozooplankton (jellyfish) biomass in the upper epipelagic zone of deep western Bering Sea region.

Pacific salmon and squid dominated the biomass of epipelagic nekton in all years. Generally speaking, chum salmon and the squid *Boreoteuthis borealis* were the most dominant species. Ratio of Pacific salmon biomass to total epipelagic nekton biomass varied between 65 % in 2007-2008 and 85 % in 2010, 2012, and 2015. Squid were the second most abundant species group and represented from 7-8 % in 2006, 2010, and 2011 to 23-25 % of total epipelagic nekton biomass in 2003, 2005, 2008, 2009, and 2014. Mesopelagic fishes were third most abundant group and represented between 0.3-2.2 % of nekton biomass.

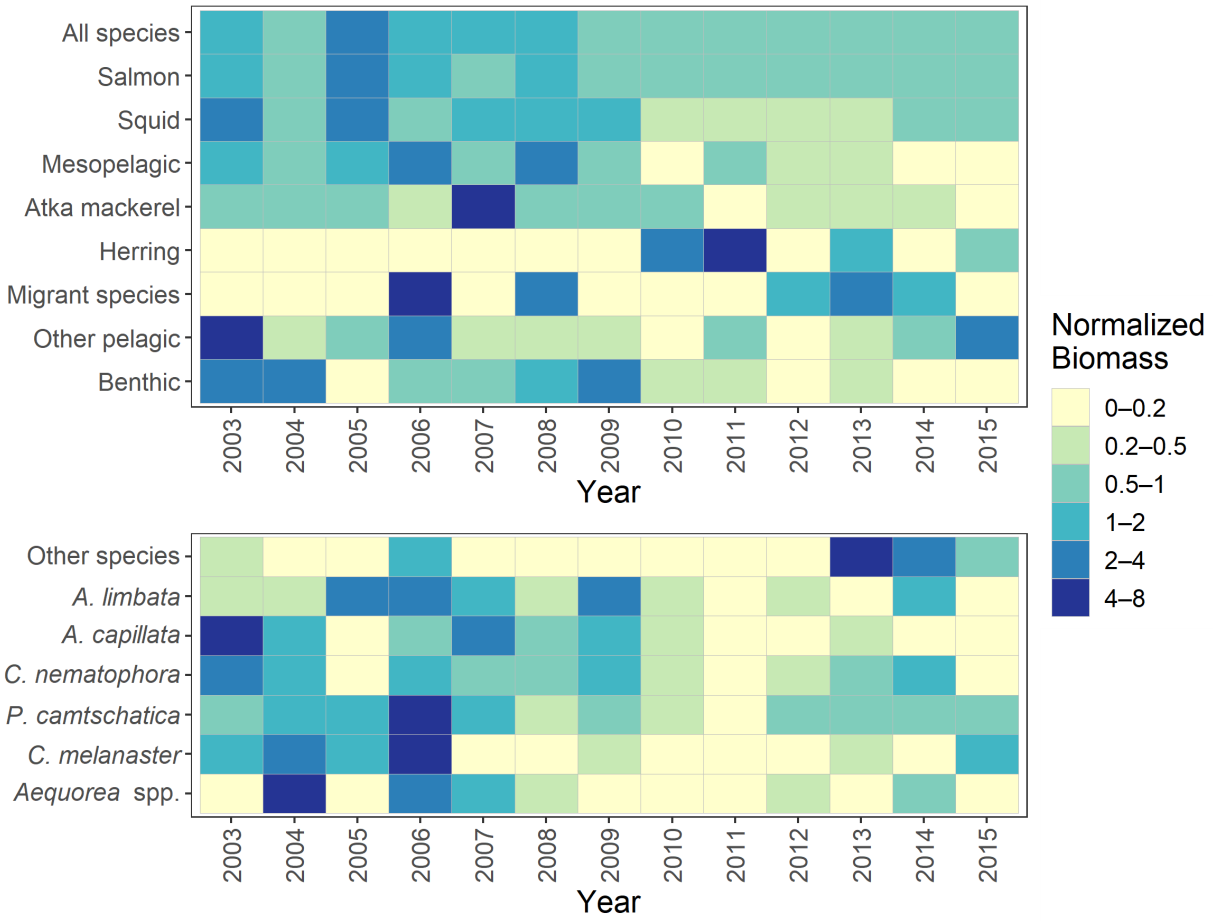

Figure R16-24. Interannual dynamics of normalized biomass (biomass divided by the multiyear mean biomass, unitless) of selected nekton (upper panel) and macrozooplankton (lower panel) taxa in the upper epipelagic layer of the western Bering Sea.

The macrozooplankton in epipelagic zone of the WBS are dominated by three taxa: the hydromedusa *Aequorea sp.* (24-92 % of macrozooplankton biomass), scyphomedusae *Chrysaora melanaster* (1-59 %) and *Phacellophora camtschatica* (2-50 %). The first taxon dominated the macrozooplankton more frequently than other two taxa, and its multiyear mean biomass contributed 75.6 % of total macrozooplankton biomass. *C. melanaster* dominated in the macrozooplankton in 2003, 2005, and 2015 and its multiyear mean biomass was about 13.6 % of total macrozooplankton. *P. camtschatica* dominated only in 2011 when the macrozooplankton biomass had the lowest value across all years (2003-2015).

Interannual changes in relative biomass of key species of nekton and macrozooplankton are summarized in Tables R16-3 and R16-4, respectively.

Table R16-3. Interannual variability of relative biomass (%) of key nekton species in epipelagic layer of the western Bering Sea.

	2003	2004	2005	2006	2007	2008	2009	2010	2011	2012	2013	2014	2015	Average
Benthic	0.1	0.2	-	-	-	0.1	0.3	0.1	-	-	0.1	-	-	0.1
Other pelagic	1.9	0.2	0.3	1.7	0.2	0.2	0.3	-	1.2	0.2	0.4	1.0	2.3	0.8
Migrants	-	-	-	3.9	-	3.0	-	-	-	2.0	3.4	2.2	-	1.0
Herring	-	-	-	-	-	-	0.2	4.3	11.4	0.1	2.9	-	1.2	1.0
Atka mackerel	0.8	1.6	0.5	0.7	9.7	0.9	1.0	1.9	0.1	0.9	0.9	1.0	-	1.5
Mesopelagic	2.2	2.1	1.1	5.5	1.9	5.3	1.6	0.7	1.8	1.5	1.0	0.5	0.3	2.2
Squid	23.6	15.2	22.5	8.5	21.7	25.0	23.0	6.7	8.7	9.4	15.4	23.0	12.5	18.2
Salmon	71.3	80.6	75.6	79.6	66.4	65.5	73.6	86.3	77.0	85.8	75.9	72.2	83.7	75.2

Note – The dashes indicate relative biomass less than 0.1.

Table R16-4. Interannual variability of relative biomass (%) of key macrozooplankton (jellyfish) species in epipelagic layer of the western Bering Sea.

	2003	2004	2005	2006	2007	2008	2009	2010	2011	2012	2013	2014	2015	Average
Other species	0	0	0	0	0	0	0	0	0	0	2.2	0.3	0.2	0.1
Aurelia limbata	0.3	0	4.1	0.3	0.5	0.3	4.2	1.5	0.6	0.4	0	0.9	0	0.4
Cyanea capillata	17.5	0.7	0	0.5	7.2	5.2	9.8	6.7	0	0.2	2.2	0.3	0	2.3
Calycopsis nematophora	15.5	0.6	1.6	1.4	1.5	5.6	13.1	9.1	2.9	2.6	6.4	3.9	1.4	2.4
Phacellophora camtschatica	8.6	1.5	20.5	7.8	6	7.4	13.2	21.9	49.6	16.5	13.4	6.1	10.4	5.7
Chrysaora melanaster	34	5.3	48.6	24.7	1.6	2.4	16.1	8.2	46.9	3.3	27.7	1	59.4	13.6
Aequorea sp.	24.1	91.9	25.2	65.4	83.2	79	43.7	52.6	0	77	48.1	87.4	28.6	75.6

8. Benthic community structure and dynamics – case study from Olyutorsky Gulf

Contributors: V.A. Nadtochii, N.V. Kolpakov, K.K. Kivva

To the best of our knowledge, the detailed information about benthic community structure is extremely sparse for the WBS region. Most of the surveys there are performed with bottom trawls and aimed at commercial stock assessment. This type of survey alone does not allow for comprehensive description of the benthic community. Here we use data of two benthic bottom-grab surveys from the Olyutorsky Gulf from 1985 and 2012. This allows us to assess benthic community structure in detail and to assess its changes over quarter of century. This section is based on the information published in Nadtochy and Kolpakov (2022).

In 1985, the work was performed aboard fisheries scientific vessel "*Mys Tihiy*" in October-November. Sixty samples were taken from depths of 20-200 m at 37 stations. The survey was repeated in August 2012 aboard R/V "*Professor Kaganovskiy*". Twenty-six stations were visited with 48 samples collected from depths 51-270 m. During both surveys samples

were collected by bottom-grab "Okean" with sampling area of 0.25 m^2. More detailed information on methodology may be found in (Nadtochy et al., 2017).

Total macrozoobenthos biomass in the study area varied between 19-3023 g m^{-2} in 1985 (581.2 ± 94.5, mean ± SD), and between 98-2428 g m^{-2} in 2012 (561.1 ± 95.2, mean ± SD). In both 1985 and 2012 sea urchins (Echinoidea), bivalves (Bivalvia), and Polychaeta dominated the biomass (Table R16-5).

Table R16-5. Mean biomass (g m^{-2}) and portion (%) of taxa in macrozoobenthos of the Olyutorsky Gulf in 1985 and 2012. Three most abundant taxa are indicated in bold.

Taxa	1985		2012	
	Biomass, g m^{-2}	Portion, %	Biomass, g m^{-2}	Portion, %
Foraminifera	+	+	3.16	0.54
Porifera	+	+	0.68	0.12
Hydroidea			1.95	0.34
Anthozoa			2.24	0.39
Actinia	2.8	0.5	8.77	1.51
Nemertini			1.05	0.18
Priapulida			1.19	0.20
Polychaeta	**44.2**	**7.9**	**62.30**	**10.72**
Sipunculida			29.45	5.07
Ostracoda			**+**	**+**
Panthopoda			+	+
Cumacea			0.19	0.03
Cirripedia	11.3	2.0	-	-
Amphipoda	2.5	0.4	1.35	0.23
Decapoda			3.78	0.65
Loricata			0.58	0.10
Solenogastres			0.01	0.002
Gastropoda	8.2	1.5	7.06	1.21
Bivalvia	**139.2**	**24.8**	**177.91**	**30.61**
Bryozoa			2.78	0.48
Brachiopoda			0.56	0.10
Asteroidea	+	+	0.02	0.004
Ophiuroidea	13.9	2.5	11.90	2.05
Echinoidea	**291.6**	**52.0**	**261.25**	**44.94**
Holothuroidea	+	+	0.04	0.01
Ascidia	24.7	4.4	2.66	0.46
Varia	22.7	4.0	0.40	0.07
Number of stations (samples)	37 (60)		26 (48)	
Area sampled (km^2)	8700		3835	
Depth range (m)	20–200		51–270	

Note – Plus signs indicate rare presence of the species, and empty cells for 1985 indicate missing data for the particular species/group.

Results revealed six and four main macrozoobenthos communities in the area of study in 1985 and 2012, respectively (Figure R16-25). Three of these main communities were the same in 1985 and 2012.

The largest community (based on prevalence across the stations sampled) was dominated by the bivalve *Macoma calcarea* in 2012. It was delineated by 11 stations and occupied most of the eastern half of the Gulf within the depth range 103-270 m. The sediments there were mud or mud with sand of varied grain size. The mean total biomass within this community was 474.0 ± 63.8 g m^{-2}. The biomass of *M. calcarea* varied between 16.8-485.4 g m^{-2} (258.0 ± 59.2 g m^{-2}, mean ± SD) and this species contributed about 44.5 % to the total biomass there. The mean biomass of bivalves there was 265.1 ± 59.2 g m^{-2} (56 %). Mean abundance of the *M. calcarea* was 26.0±5.1 ind. m^{-2}. Besides bivalves, this community consisted of another 21 taxa with most dominant taxa being Polychaeta and Sipunculida. In 1985, this community almost entirely occupied the outer part of shelf in the depth range 100-180 m. It was evident at 10 of 37 stations. The mean biomass of the community was 445.3 ± 80.5 g m^{-2}. The biomass of the *M. calcarea* was 18.4-660.0 g m^{-2} with a mean ±SD of 208.5 ± 64.4 g m^{-2} (46.8 % of total biomass). In 1985, this community was also dominated by bivalves *Tridonta elliptica*, sea urchin *Strongylocentrotus pallidus* and Sipunculida.

Another large community in the Olyutorsky Gulf is dominated by the sea urchin *S. pallidus*. It was present at 6 stations in 2012 and 7 stations in 1985. In 2012, mean total biomass within this community was 417.3 ± 45.6 g m^{-2}. Biomass of the *S. pallidus* varied between 4.2-373.8 g m^{-2}. Its mean biomass was 167.9 ± 39.6 g m^{-2} (40.2 % of total mesozoobenthos biomass). Mean abundance of the *S. pallidus* was 12.0±3.4 ind. m^{-2}. This community also included 19 other taxa, most abundant of which were bivalves and Polychaeta.
This community was also abundant in 1985. Mean total biomass within this community was 434.8 ± 159.3 g m^{-2} in 1985. Biomass of the *S. pallidus* varied between 18.4-866.0 g m^{-2} with mean ± SD 252.0 ± 104.3 g m^{-2} (58 % of total biomass). The bivalve *Macoma calcarea* was also abundant in this community in 1985.

The third main community in 2012 was dominated by the sand dollar *Echinarachnius parma*. It occupied 6 stations in 2012 and 12 stations in 1985. This community is confined mostly to sand sediments or sand with gravel. The mean total biomass in this community was 1045.6 ± 342.3 g m^{-2}. The biomass of the *E. parma* was 98.1-2428.9 g m^{-2} with a mean value of 868.6 ± 347.6 g m^{-2}. This is roughly 83 % of the total biomass. The mean abundance of this species was 109.6 ± 41.1 ind. m^{-2}. This community also included animals of 14 other taxa. The most dominant taxon was bivalves. Polychaeta was the third most dominant taxon there, though its biomass was substantially lower in the community than Bivalvia. This community was the largest in 1985, though it covered mostly inner and middle shelf with depths between 20-110 m which were not sampled in 2012. In 1985, this community occupied 12 stations. Its mean biomass was 806.6 ± 274.3 g m^{-2}. The key species biomass was 98.1-2428.9 g m^{-2} with mean ± SD value of 605.0 ± 263.2 g m^{-2}. Besides sand dollar, the most abundant species in this community were bivalves *M. calcarea* and *Cyclocardia crebricostata*.

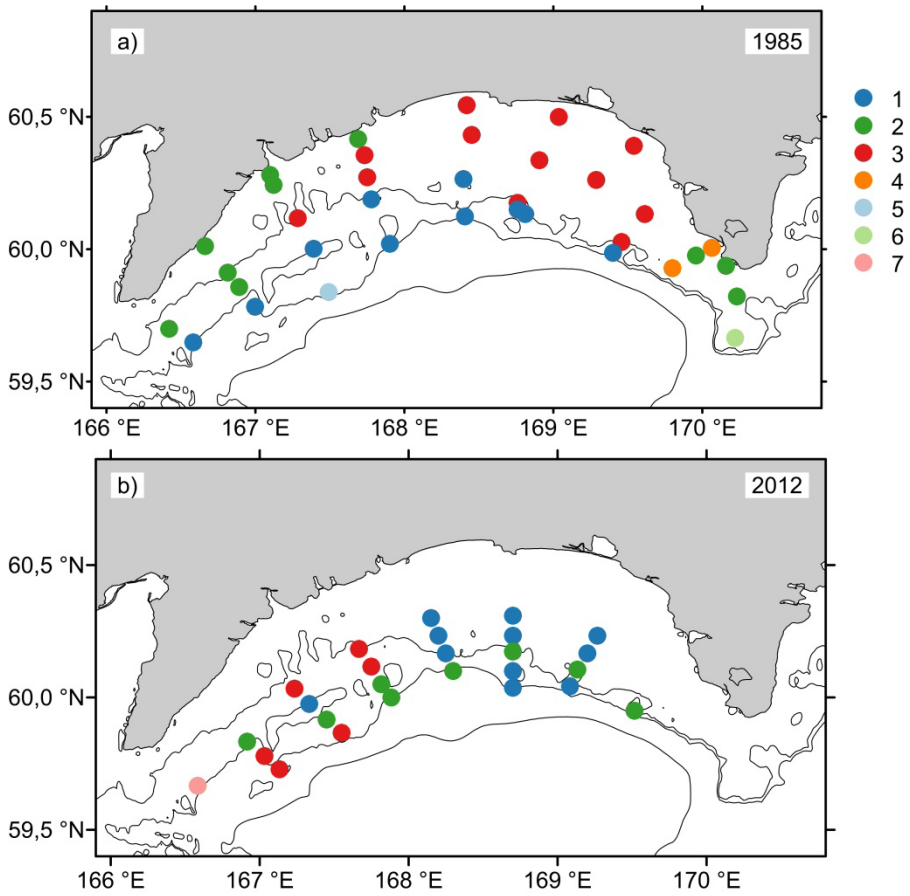

Figure R16-25. Main macrozoobenthic communities in the Olyutorsky Gulf in 1985 (a) and 2012 (b). Communities were dominated by: 1 – *Macoma calcarea*; 2 – *Strongylocentrotus pallidus*; 3 – *Echinarachnius parma*; 4 – Cirripedia; 5 – Polychaeta; 6 – *Ophiopholis aculeata*; 7 – *Chlamys albida*. Solid lines represent isobaths 100, 200 and 2000 m based on GEBCO.

All other communities were sampled only in 1985 or 2012 probably due to the differences in the area of sampling. Three smaller communities were present in 1985, but not in 2012. Those include a community dominated by barnacles (Cirripedia) with large portion of epifauna (sponges and soft corals Gersemia). This community was located in the eastern part of the polygon close to Cape Olyutorsky. Polychaeta was the dominant taxon in one station in 1985 located in the outer shelf at a depth of 180 m. Also, one station had crevice brittle star *Ophiopholis aculeata* as its dominant species. It was located south of Cape Olyutorsky.

The fourth community of 2012 was dominated by scallop *Chlamys albida*. It was sampled only on one station in the very western portion of polygon on depth of 119 m. The sediment there was muddy sand with addition of gravel and pebbles. The mean total biomass there was 287.6 g m^{-2} with the key species biomass of 144.0 g m^{-2} (50 %). Mean abundance of the key species was 2 g m^{-2}. There were 11 other taxa in the community, with dominance in biomass by sea squirts (Ascidae), Polychaeta, and Decapoda.

Some redistribution of macrozoobenthos communities obviously occurred in the Olyutorsky Gulf between 1985 and 2012. *M. calcarea* spread northward to the inner shelf and lost

dominance in the middle shelf in the eastern part of gulf. The sea urchin *S. pallidus* became the dominant species in a narrow band of the middle shelf. It is impossible to conclude if this taxon is still abundant in the eastern near shore area and near Cape Olyutorsky as sampling was not performed there in 2012. The sand dollar *E. parma* was observed to be the dominant taxon in the eastern outer shelf of the polygon. However, those locations were mostly not sampled in 1985. So, it is difficult to conclude if this is due to sampling or species redistribution. However, the main communities did not change significantly in the Gulf of Olyutorsky area between 1985 and 2012 both in terms of species composition and mean biomass.

9. Fisheries in the region

Contributors: A.O. Zolotov, N.V. Klovach, K.K. Kivva

The shelf and shelf break areas along the eastern Kamchatka and the western Bering Sea are historical regions of intensive fisheries. Other types of commercial use of the ecosystems, including oil and gas mining, are not developed in the region. Therefore anthropogenic pressure there exists mostly in form of selective harvesting of living marine resources.

For management purposes, the region is divided into three large areas (zones). East Kamchatka fishing area expands from Cape Lopatka in the south to Cape Olyutorsky in the north. It is subdivided into Petropavlovsk-Komandorsky subarea and north-eastern Kamchatka (Karaginsky) subarea. The third statistic area is called Western Bering. It expands from Cape Olyutorsky on the west to the US-Russia convention line on the south and to the 175° W on the east (Figure R16-26). Despite this area spanning most of the Gulf of Anadyr, we use the numbers for this area in our report because there are no other reliable long-term statistics data for smaller subareas.

Those three areas together are relatively significant in terms of fisheries. In 2009-2016, they accounted for about 27 % of total annual catch of fishes and about 19 % of total annual catch of invertebrates in the Far Eastern part of Russia. At the same time, total catch there increased from about 570,000 tonnes in 2009 to about 830,000 t tonnes in 2016 (Figure R16-26).

The most important commercial species of east Kamchatka and western Bering Sea are quite traditional for the Far Eastern region of Russia as a whole. The basis of marine fisheries includes walleye pollock (*Theragra chalcogramma*), Pacific herring (*Clupea pallasii*), Pacific cod (*Gadus macrocephalus*), Pacific salmon (*Onchoryncus* spp.), Atka mackerel (*Pleurogrammus monopterygius*), grenadier (*Macrourus* spp.) and cephalopods. In 2009-2016, those species together contributed about 481, 72, 50, 14, 12 and 22 thousand tonnes to mean total annual catch, respectively. Their overall contribution to regional fisheries is more than 90 % by weight. Coastal fisheries rely mostly on Pacific salmon (*Onchoryncus* spp.), flounders (*Pleuronectiformes* spp.), sculpins (*Scorpaeniformes* spp.), and saffron cod (*Eleginus gracilis*). They contribute about 3.7, 2, 2, and 1 % of total annual catch in the region, respectively. On the other hand, the contribution of the most commercially important species including crabs and prawns is relatively small. In 2009-2016 their catch was less than 1 % of the total catch by weight.

Because the salmon fishery and catch reporting are organized quite differently in Russia compared to other oceanic fisheries, in this report we separate information on the salmon fishery from other fishery statistics.

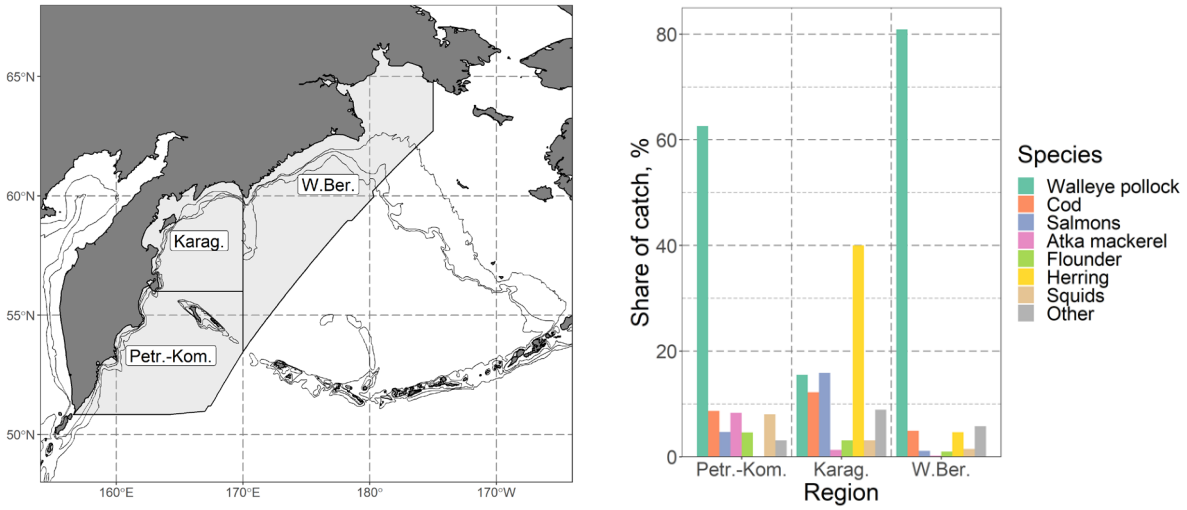

Figure R16-26. Catch structure (%) in 2009-2016 in Pacific waters of Kamchatka and western Bering Sea. Left panel – fishery statistical areas (subareas) of the western Bering Sea region (Petr.-Kom. – Petropavlovsk- Komandorsky, Karag. – Karaginsky, W.Ber. – Western Bering). Right panel – share of mean catch of different species (%) in three areas related to the western Bering Sea region.

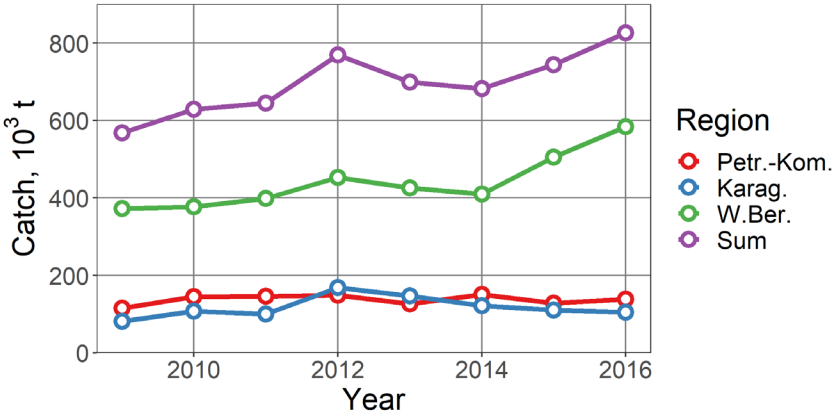

Figure R16-27 Total catch dynamics (10^3 tonnes) in 2009-2016 in Pacific waters of Kamchatka and western Bering Sea. The data represent three fishery areas (subareas): Petr.-Kom. – Petropavlovsk- Komandorsky, Karag. – Karaginsky, and W.Ber. – Western Bering; see figure R16-25 for location of areas.

9.1. Non-salmon fisheries

Overall catch statistics for the described areas reveal variable but generally stable catches there (Figure R16-27). However, the catch of particular species was notably variable (Figure R16-28). During the past few decades a substantial decrease in walleye pollock catches was observed in all three areas (or subareas). It is most pronounced in the Western Bering area; the catches dropped there from about 800-1000 thousand tonnes in the 1980s to about 200-400 thousand tonne in recent years (not shown). Note however that walleye

pollock stock mostly lies west to the Cape Navarin and main catches of this species occur there (Stepanenko and Gritsay, 2016; 2018), so in terms of this report they belong to the Northern Bering Sea region (region 14, see figure R16-1). Walleye pollock catches in the Petropavlovsk- Komandorsky subarea has also dropped from relatively high values of over 100,000 tonnes in late 1980s to values below 50,000 tonnes in 2000-2005. However, the walleye pollock catch has recovered there recently and was in the range of 80,000-93,000 tonnes in 2010-2015. Walleye pollock fisheries are also decreasing in the Karaginsky subarea. There was also a decrease in Atka mackerel catches in Petropavlovsk-Komandorsky subarea in 2010-2016. Flounders demonstrate relatively low though stable catches in both the Petropavlovsk- Komandorsky and Karaginsky subareas. On the other hand, there was a substantial increase in Pacific herring catches in Karaginsky subarea in 2012-2016. Moreover, published data allow us to conclude that there is an increase in catch of halibut, grenadier, Atka mackerel, sculpin (Cottoidea), ray, smelt fish (Osmeridae) and rockfish in the Russian part of the Bering Sea in 2000-2016 compared to the previous century (Datsky, 2019b).

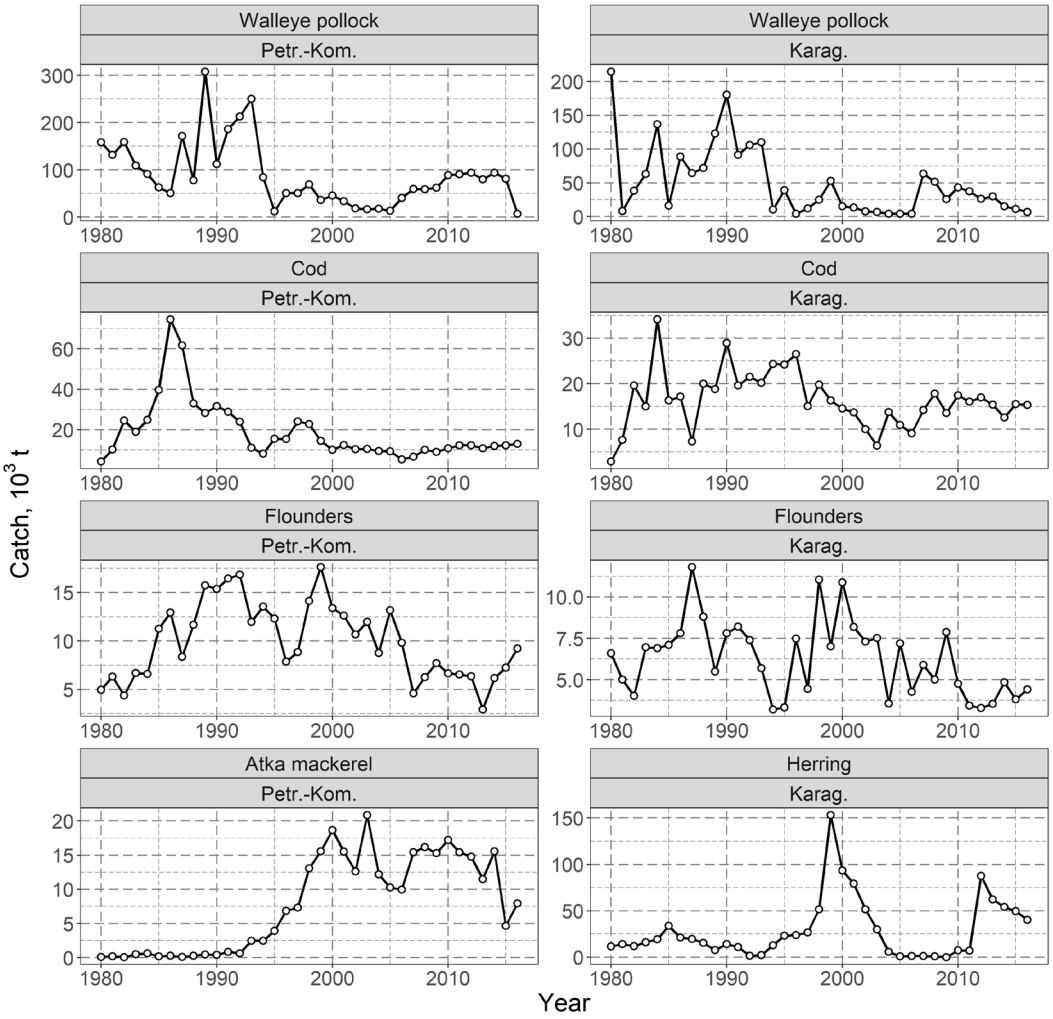

Figure R16-28. Catch dynamics of the main commercial non-salmon species (thousand tonnes) in the Petropavlovsk-Komandorsky (left panels) and Karaginsky (right panels) subareas of the east Kamchatka fishery area in 1980-2016. See figure R16-25 for location of areas. Note different scales of y-axis in different panels.

9.2. Salmon fisheries in the region

Three main species of Pacific salmon are responsible for more than 95 % of the total catch of salmons in the Far Eastern part of Russia. Those species are pink salmon (*Oncorhynchus gorbuscha*), chum salmon (*O. keta*), and red or sockeye salmon (*O. nerka*). The same species dominate the salmon communities in the eastern Kamchatka region in particular. This region from Cape Navarin in the north to Cape Lopatka (the southernmost cape of the Kamchatka Peninsula) in the south contributes more than half of the total salmon catch in Russia. More than 95 % of this catch is supported by natural reproduction. Only three salmon hatchery farms are located in this region and they release mostly chum salmon.

There are more than 135 spawning salmon rivers in this area. 50 of them are located on the Pacific Ocean coast (Petropavlovsk-Komandorsky subarea), and more than 85 run into the Bering Sea (Karaginsky subarea). The north-eastern coast of Kamchatka serves as the main spawning area for pink salmon in the region. In 2009-2016, 96.2 % of total pink salmon catch in the region occurred there in the north-eastern part (Karaginsky subarea). The rivers of the Karaginsky Gulf of the Bering Sea are the most important pink salmon spawning rivers there (Antonov, 2011).

Despite the fact that pink salmon catch in the north-eastern Kamchatka is 5-30 times higher than in the south-eastern Kamchatka, stock dynamics are similar in those two areas. This is because the number of pink salmon coming to as well as caught in the Kronotsky and Avachinsky Gulf (eastern coast of the Kamchatka Peninsula) are strongly affected by straying of pink salmon from the Karaginsky Gulf into the Kamchatsky Gulf.

The interannual changes in pink salmon catch are relatively large (Figure R16-29), and maximum catches occur in odd years. The historic highest catch of pink salmon in the eastern Kamchatka has occurred in 2009 (135,200 tonnes) and 2011 (177,700 tonnes). The corresponding abundance of this species was evaluated to be in range of 205-220 million individuals (Shevlyakov et al., 2009; Shevlyakov et al., 2016). The mean catches during odd years from 2009-2015 is 111,800 tonnes, which is about 2 times higher than the mean catch during odd years from 2001-2007.

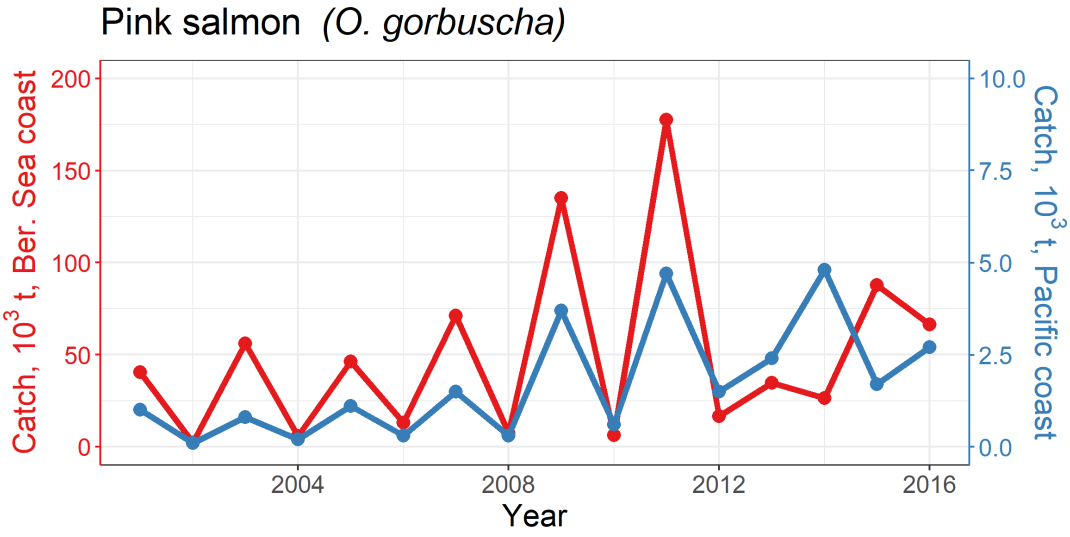

Figure R16-29. Catch dynamics (thousand tonnes) of pink salmon in the western Bering Sea region including Bering Sea coast (left axis, red, Petropavlovsk-Komandorsky subarea) and Pacific Ocean coast (right axis, blue, Karaginsky subarea).

Fluctuations in the abundance of pink salmon in the region are ruled mostly by climatic changes. For example, the cold ocean winter conditions of 2012-2013 resulted in a decrease of overwintering survival and catch of pink salmon in 2013 and 2014. On the other hand, the warm ocean conditions of the El Niño of 2015 led to an increase of survival and higher catch of this species in 2016 (Kotenev et al., 2015).

The east coast of the Kamchatka Peninsula is the one of most important regions for chum salmon reproduction in the Far Eastern region of Russia. Chum salmon are the second most abundant salmon species in the region, and it is the most abundant one in some even years.

The main spawning rivers of chum salmon of north-eastern Kamchatka run into Karaginsky Gulf. In the Olyutorsky Gulf area, the main spawning rivers are the Pakhacha and the Apuka. Along the Pacific coast of the Kamchatka Peninsula, reproduction and fisheries of chum salmon mostly occur in the basin of Kamchatka River. The other important spawning rivers are the Zhupanovka River and rivers of the Avachinsky Gulf.

Total catch of chum salmon in the region in 2009-2016 varied between 8,700 tonnes to 28,100 tonnes in 2011 and 2014, respectively (Figure R16-30). The mean catch for 2009-2016 was 15,100 tonnes per year. The largest part of the catch was contributed by north-eastern part of Kamchatka coast (6,400-21,100 tonnes), and only one third to one fourth was contributed by the Pacific coast of the peninsula (2,300-7,000 tonnes depending on year). For comparison, catch of chum salmon in 2001-2008 varied from 4,000-12,400 tonnes and the mean catch was 8,600 tonnes.

Similar to pink salmon, the stock and catch of chum salmon increased during the early 2000s. They reached their maximum in 2014 and started to decrease after the pink salmon stock has decreased (with lag of 4-5 years corresponding life cycle).

Abundance of chum salmon breeds is determined by abundance of post-spawning adults as well as total abundance of post-spawning salmon. Pink salmon usually contributes the largest part of total post-spawning salmon. The material of post-spawning fishes supports oligotrophic rivers of Kamchatka peninsula with organic matter which in turn contributes to the food items of juvenile chum salmon (Shevliakov and Zavarina, 2004).

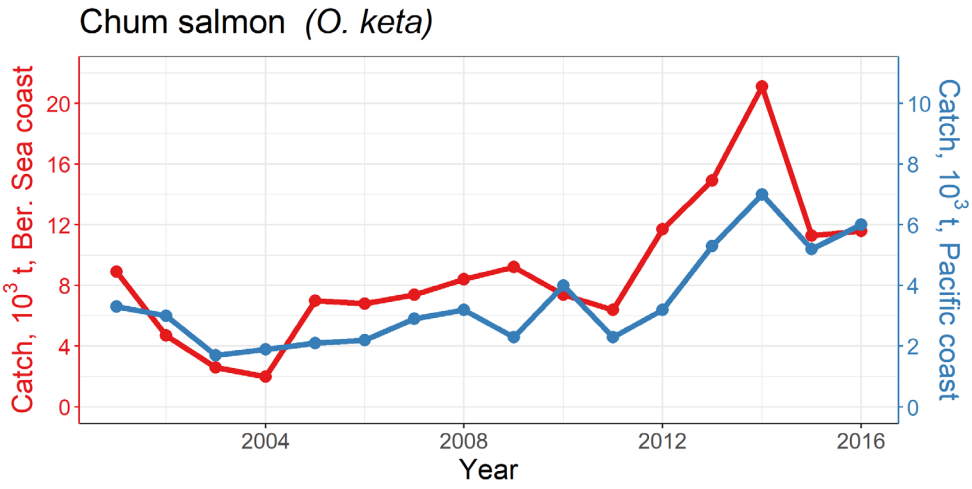

Figure R16-30. Catch dynamics (thousand tonnes) of chum salmon in the western Bering Sea region including Bering Sea coast (left axis, red, Petropavlovsk-Komandorsky subarea) and Pacific Ocean coast (right axis, blue, Karaginsky subarea).

The abundance of pink salmon influences the growth rate and maturing rate of chum salmon as both of those species feed in similar areas in the Bering Sea. This is suggested by (Zavarina, 2008) who made the comparison of age structure of adult salmons during long-term periods of high and low abundance. In the 1980s there was a low abundance of salmon in Apuka River and fish of age 3+ were dominant. After the subsequent rise of chum and pink salmon abundance, chum salmon returned mostly at age 3+ or 4+ depending on the year. In 2009-2016, most returning chum salmon were age 3+ or 4+. In even years with high abundance of pink salmon, the mean age of spawning chum salmon was higher than in odd years. This supports the hypothesis of density factors influencing the chum salmon during the feeding period. As a result, in even years, a considerable part of the chum salmon population postpones their return for spawning and returns in the subsequent odd year (Klovach and El'nikov, 2013).

Sockeye salmon stocks of the eastern coast of Kamchatka were relatively high in 2009-2016 (Figure R16-31). This has supported a mean catch of 13,200 tonnes per year (9,600-18,000). For comparison, sockeye salmon catch in the region in 2001-2008 was from 2,900-7,200 tonnes.

Unlike pink and chum salmon, the main spawning rivers of the sockeye salmon are located along the Pacific coast of the Kamchatka Peninsula. The most important spawning area is the Kamchatka River basin.

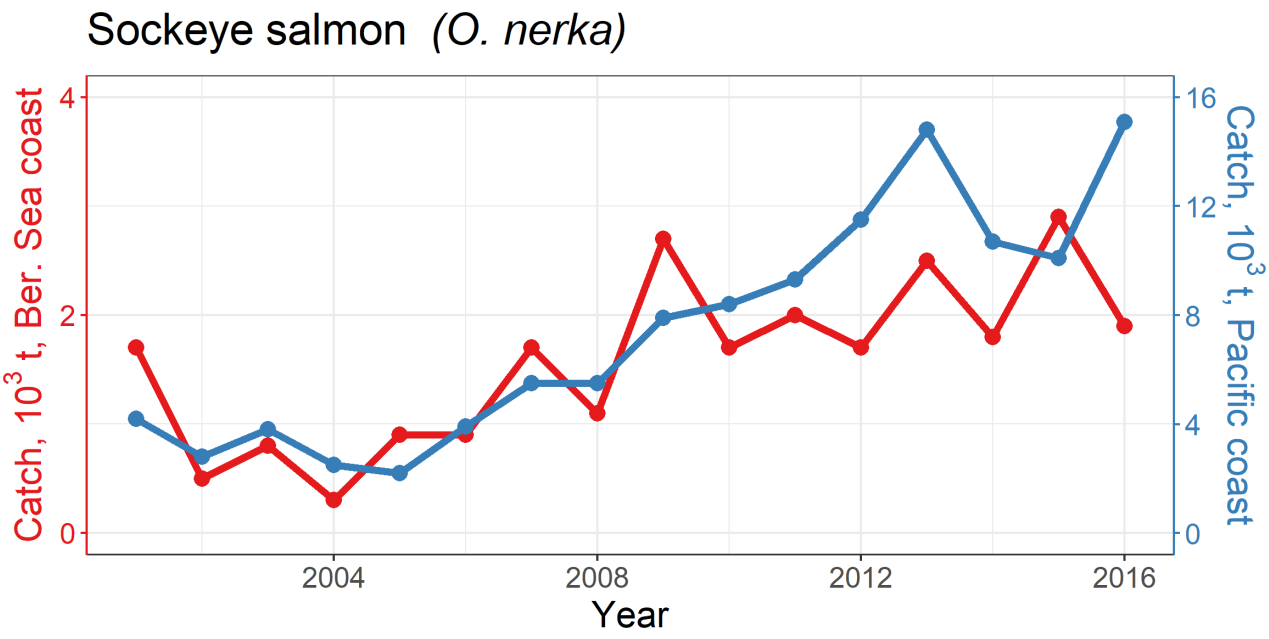

Figure R16-31. Catch dynamics (thousand tonnes) of sockeye salmon in the western Bering Sea region including Bering Sea coast (left axis, red, Petropavlovsk-Komandorsky subarea) and Pacific Ocean coast (right axis, blue, Karaginsky subarea).

10. Contaminants

Contributors: M.V. Simokon, L.T. Kovekovdova

The Bering Sea is one of the commercially important fisheries regions in the PICES area. The quality and safety characteristics of marine living resources are directly connected to the quality of their environment. Contamination of the environment with chemical compounds could lead to biological accumulation of those contaminants in the tissues of marine fish and animals (Wcislo et al., 2008).

Sources of marine contamination vary greatly. Organic pollutants are introduced to the marine environment mainly by human activities. On the other hand, metals are natural elements which may have natural as well as anthropogenic sources (Censi et al., 2006). Biogeochemical cycles of some elements are affected by their sources. Natural sources of heavy metals are outflow, aeolian deposition, and hydrothermal activity. Anthropogenic sources such as wastewater, waste dumping, and ship-based sources play a bigger role in the coastal areas.

Both deficits and excess of microelements in the marine environments may negatively affect marine organisms (Hunter et al., 1997). Trace metals Fe, Cu, and Cd are essential for phytoplankton production (Morel and Price, 2003; Lane et al., 2005). On the other hand, Cu and Cd may be toxic (Brand et al., 1986; Tortell and Price, 1996). In the subarctic Pacific, Fe is major limiting element for phytoplankton primary production (Takeda and Tsuda, 2005). Thus, microelement composition of the sea water plays an important role in ecosystem functioning.

Samples of contaminants and trace metals were collected in the western Bering Sea region during summer cruises of TINRO in 2011-2016. Samples were collected in 1 L glass bottles, acidized to pH = 1-2, and analyzed in the stationary laboratory in TINRO with atomic absorption and mass spectroscopy methods.

Observed ranges of trace metals in the western Bering Sea were (μg l^{-1}): As – 0.3-19.6; Cd – 0.08-0.329; Co – 0.024-1.83; Cr – 0.2-13.3; Cu – 1.24-10.03; Fe – 3.97-27.3; Hg – 0.022-0.15; Mn – 0.4-138.6; Ni – 0.40-1.27; Pb – 0.1-3.13; Zn – 4.8-34.7.
An example of spatial distribution of Hg is given in Figure R16-32.

According to Russian law, threshold levels (maximum allowable concentration) for trace metals in fishery water bodies are (μg l^{-1}): As – 10; Cd – 10; Co – 5; Cr – 20; Cu – 5; Fe – 100; Hg – 0.1; Mn – 50; Ni – 10; Pb – 10; Zn – 50. Thus, threshold levels were exceeded in the western Bering Sea occasionally for As, Cu, Hg, and Mn. Nevertheless, environmental conditions of the region are generally clean in terms of trace metals.

Correlation analysis revealed groups of trace metals with similar distribution. Significant correlation was observed amongst As, Cd, Co, Cr, Cu, Fe, Pb and Zn. The concentrations of Mn and Ni were also significantly correlated. Mercury (Hg) showed no correlation with other trace metals. This reflects different pathways of contamination or natural sources. While Fe and its concomitant elements come to the sea mostly through river runoff, the main source of mercury (Hg) may be aeolian transport and deposition.

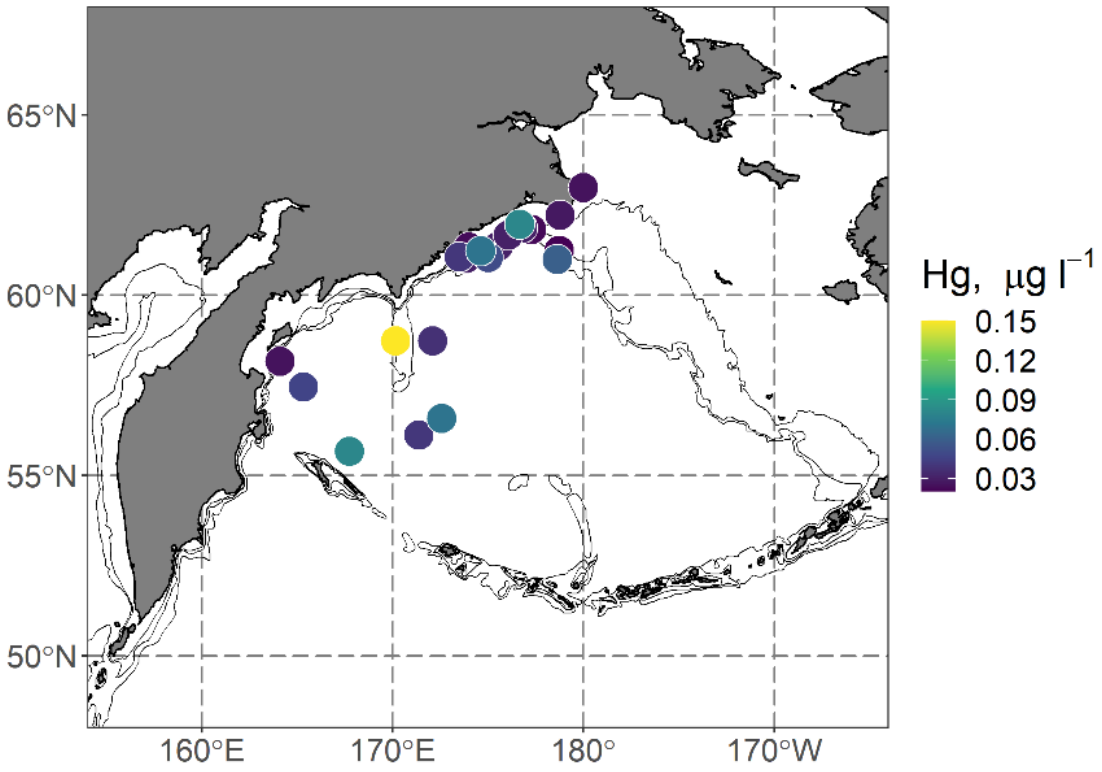

Figure R16-32. Spatial distribution of Hg (µg l^{-1}) in the upper layer of the western Bering Sea. Note the figure combines data from June-September of 2011-2017. The highest value (0.15 µg l^{-1}) was observed in June 2011. All other values are below 0.08 µg l^{-1}.

Concentrations of persistent organic pollutants in the western Bering Sea are less than the limit of detection for used methods.

11. Conclusion

This report combines available published information and some unpublished data on the structure and dynamics of both abiotic and biotic parts of the large marine ecosystem of the western Bering Sea with particular emphasis on their variability during 2009-2016. As this is one of the first attempts to fully describe the WBS ecosystem, we tried to put the data into broader context and present the information on previous years when possible. To the best of our knowledge, multiple sections of this report provide information which is published in English for the first time. These include seasonal and interannual variability of dissolved oxygen and dissolved inorganic nutrients content; the data on zooplankton community structure dynamics in the 0-200 m in 1986-2018; multiyear mean nekton community of the epipelagic layer (roughly 0-40 m) as well as dynamics of nekton community in 2003-2015; comparison of the benthic community in the Olyutorsky Gulf between 1985 and 2012; and general information on contaminants in the upper layer of the sea.

We demonstrate significant variability in the physical setup of the WBS ecosystem and recent trends to warming of the surface layer as well as deeper layers. The upper 50 m of the water column are almost consistently warmer than mean for 1950-2000 since 2002. Despite the reported slightly negative or zero temperature anomalies for 50-150 m layer in 2006-2007 and the 50-300 m layer in 2008-2013, this cold event has changed to consistent warming since 2014 and deeper waters (400-1000 m) are also consistently warmer than reference values for 1950-2000 since 2006. The salinity of the surface layer shows a generally decreasing trend from 2003-2014. Sea surface temperature data suggest that the WBS as a whole is in a generally warm state since 2003. Since 2014, there were multiple winter and summer months with SST larger than multiyear mean plus one standard deviation. Altogether this illustrates the severity of long-term changes in the physical setup of the WBS ecosystem. We believe most of those changes are related to the state of the North Pacific and are also translated further north to the northern Bering Sea and Chukchi Sea.

Despite these obvious trends in the physical setup, we do not see a clear linear connection of other parts of the ecosystem to those changes. For example, analysis of the chlorophyll-a concentration dynamics reveals later phytoplankton blooms in the area close to Cape Navarin since 2013 and earlier blooms near Kamchatka Strait since 2009. The inconsistency of those trends with general trends in temperature and salinity is due to non-linear dependence of the phytoplankton community on physical conditions such as winter and spring mixing, solar radiation, sea ice distribution and melt etc. (Kivva and Kubriakov, 2021).

Since 2012, we see consistent increase of zooplankton biomass in the WBS. This is mostly ruled by an increase in the Chaetognatha (arrowworms) biomass. However, this result should be treated with caution because for the purposes of this report we combined data on zooplankton from June-October, so in some years there may be a bias due to seasonal variability of the community. At this stage it is hard to confidently conclude if those apparent changes in the zooplankton community are attributed to the warming of the WBS, but this seems to be a reasonable explanation. Warmer conditions may theoretically lead to better over-wintering of chaetognaths in the deep area of the sea. Another possible factor influencing the zooplankton community in this area may be water circulation which can significantly change on decadal time scales. However, we currently lack the information on recent variability circulation in the area.

The available data allowed us to demonstrate seasonal changes in the nekton community structure of the upper epipelagic layer. We show that salmon (mostly immature chum) dominate the biomass from end of July to beginning of October. The second dominant taxon

of this layer are squids, the most abundant of which are *Boreoteuthis borealis* and *Gonatus kamtschaticus*. Mesopelagic species also contribute a significant portion of the nekton biomass in this layer in July-September. This information illustrates a potential signal of seasonality in the survey results.

The surveys were made in approximately same time of the year in 2003-2015 (but see table 1 in Somov, 2017) which allowed us to compare results and reveal interannual variability in fish community structure. According to summer-autumn surveys, the biomass of nekton has decreased in the WBS since 2010. There was a particular decrease in biomass of all dominant taxa, as well as Atka mackerel and benthic species. On the other hand, Pacific herring and southern migrants such as Pacific pomfret, Pacific saury, Pacific spiny dogfish, and Japanese anchovy were in general more abundant than usual in 2010-2015. The same surveys showed an increase in gelatinous zooplankton in the area in recent years (2012-2015).

The most important commercial fish species in the region are walleye pollock, Pacific cod, Atka mackerel, Pacific herring, and three species of Pacific salmon: pink, chum, and sockeye salmon. The catches of pollock have decreased in the Karaginsky subarea of the region, though the catches of herring have substantially increased. The catches of salmon are also increasing in the recent years. Other main species show generally stable catches. Compared to the data up to the early 2000s there is also an increase in the catch of halibuts, macrouruses, Atka mackerel, sculpins (Cottoidea), rays, and smelt fishes (Osmeridae) (Datsky, 2019b).

The available data on trace metals and persistent organic pollutants show that the WBS environment is currently generally clean and safe in terms of chemical contamination. However, the research focused on contamination there is sparse.

According to existing publications, marine mammals represent quite a significant part of the ecosystem in the north-west part of the Pacific Ocean and particularly in the western Bering Sea (Shuntov and Ivanov, 2015). Despite regular research on the marine mammals, at least on the Commander Islands (e.g., Mamaev, 2018), we were unable to find recent overviews of marine mammal abundance and dynamics in the WBS in order to include this information into this report. The data or syntheses on marine birds' dynamics are also currently lacking for the WBS area. Finally, we are unable to synthesize information on ecosystem services or human dimensions in the region currently. The attempts to incorporate this kind of information into the status reports of the western Bering Sea could be made during further work.

Information on chemical species spatial variability is extremely sparse and incomplete in the region. The available chemical data covers dissolved oxygen, silicate and phosphate, but measurements of inorganic nitrogen species are very seldom, and data on carbonate system or organic matter composition is virtually absent. Phytoplankton composition or primary productivity peculiarities are studied in the region only sporadically, and to the best of our knowledge there were no such research efforts in 2009-2016. Therefore, many sections of this report are poorly supported with *in situ* data. We wish this situation may change with time as the information on lower trophic levels is crucial for understanding of the ecosystem changes including commercial stocks dynamics.

Nevertheless, the large portion of this report is based on data from regular fisheries surveys conducted in the WBS. We were able to conclude on substantial large-scale temporal change in the zooplankton and fish communities which are most likely attributed to changes in the physical setup of the ecosystem. Therefore, we would like to highlight the necessity of continuation and widening of those regular surveys.

Finally, we would like to express sincere gratitude to PICES Secretariat for emphasizing the work on this report and specifically to PICES WG-35 members for valuable discussions on the earlier versions of this report.

12. References

Antonov, N.P. 2011. Commercially harvested species of fish of the Kamchatka Region: biology, stocks and fisheries. Moscow, Russia: VNIRO. 245 p.

Bajtalyuk, A.A., Davydova, S.V. 2002. Distribution and passive migrations of saury in the North Pacific Ocean. Vopr. rybolovstva. 3(11): 402-420. (In Russian).

Baker, M.R., Kivva, K.K., Pisareva, M.N., Watson, J.T., Selivanova, J. 2020. Shifts in the physical environment in the Pacific Arctic and implications for ecological timing and conditions. Deep Sea Research Part II: Topical Studies in Oceanography 177: 104802.

Basyuk, E.O. 2011. Interannual variability of temperature anomalies in the water column of the western Bering Sea from 1950-2010. Fisheries Oceanography Issues 8-1: 125-147. (In Russian).

Belkin, I.M. 2016. Comparative assessment of the West Bering Sea and East Bering Sea large marine ecosystems. Environmental Development 17: 145-156.

Borisov, B.M., Volkov, A.F., Gorbatenko, K.M., Koval, M.V., Shershneva, V.I. 2004. Standard tables of the wet weight and some biochemical parameters (caloriecontent, fats, proteins, carbohydrates, and the mineral rest) of zooplankton in the Far East Seas. Izvestia TINRO 138: 355-367. (In Russian).

Bower, J.R., Takagi, S. 2004.Summer vertical distribution of paralarval gonatid squids in the northeast Pacific. Journal of plankton research 26(8): 851-857.

Brand, L.E., Sunda, W.G., Guillard, R.R.L. 1986. Reduction of marine phytoplankton reproduction rates by copper and cadmium. J. Exp. Mar. Biol. Ecol. 96(3): 225-250.

Bugaev, A.V. 2007a. Bering-Aleutian salmon international survey (BASIS): population-biological studies. Part 2 - Sockeye Salmon *Oncorhynchus nerka*. Izvestia TINRO 151: 153-187. (In Russian).

Bugaev, A.V. 2007b. Bering-Aleutian salmon international survey (BASIS): population-biological studies. Part 3 - Chinook Salmon *Oncorhynchus tschawytscha*. Izvestia TINRO 151: 188-205. (In Russian).

Bugaev, A.V., Zavolokina, A.A., Zavarina, L.I., Shubin, A.I., Zolotukhin, S.F., Kaplanova, N.F., Volobuev, M.V., Kireev, I.N. 2007. Bering-Aleutian salmon international survey (BASIS): population-biological studies. Part 1 - Chum salmon *Oncorhynchus keta*. Izvestia TINRO 151: 115-152. (In Russian).

Censi, P., Spoto, S.E., Saiano, F., Sproveri, M., Mazzola, S. 2006. Heavy metals in coastal water system. A case study from North Western Gulf of Thailand. Chemosphere 64: 1167-1176.

Datsky, A.V., 2019a. The raw material base of fisheries and its use in the Russian waters of the Bering Sea. Message 2. Interannual dynamics of the projected and actual catch of aquatic biological resources at the present stage and in historical perspective. Trudy VNIRO. 175. 130-152.

Datsky, A.V., 2019b. The raw material base of fisheries and its use in the Russian waters of the Bering Sea. Message 2. Interannual dynamics of the projected and actual catch of aquatic biological resources at the present stage and in historical perspective. Trudy VNIRO. 177. 116-122.

Gershanovich, D.E. 1963. Bottom relief of the fishing grounds and some features of the Bering Sea geomorphology. In Soviet fisheries investigations in the North-Eastern part of the Pacific Ocean, Part 1. Moscow, Russia: 13-76. (In Russian).

Glebov, I.I., Khoruzhiy, A.A., Matveev, V.I. 2010a. Features of nekton community composition in the upper epipelagic layer of the western Bering Sea in early summer. Izvestia TINRO 162: 61-76. (In Russian).

Glebov, I.I., Savinykh, V.F., Baitalyuk, A.A. 2010b. Subtropical Migrants in the Southwestern Part of the Bering Sea. Journal of Ichthyology 50(6): 430–444.

Glebov, I.I., Sviridov, V.V., Ocheretyanny, M.A., Efimkin, A.Ya., Slabinsky, A.M., Basyuk, E.O. 2004. Description of nekton and plankton communities of the upper epipelagic layer in the western Bering Sea and Pacific waters off Kamchatka in summer 2003. Izvestia TINRO 139: 43-60. (In Russian).

Hood, D.W., E.J. Kelley. 1974. Introduction: Summary of early exploration and oceanographic features, pp. xv-xxi, In Oceanography of the Bering Sea with emphasis on renewable resources. Inst. Mar. Sci., Univ. of Alaska, Alaska, Fairbanks.

Hughes, F.W., Coachman, L.K., Aagard, K. 1974 Transport and water exchange in the western Bering Sea. In Hood, D.W., Kelly, E.J. Oceanography of the Bering Sea: 59-98. Fairbanks: Institute of Marine Science, University of Alaska.

Hunt, G.L, Jr., Allen, B.M., Angliss, R.P., Baker, T., Bond, N., Buck, G., Byrd, G.V., Coyle, K.O., Devol, A., Eggers, D.M., Eisner, L., Feely, R., Fitzgerald, S., Fritz, L.W. Gritsay, E.V., Ladd, C., Lewis, W., Mathis, J., Mordy, C.W., Mueter, F., Napp, J., Sherr, E., Shull, D., Stabeno, P., Stepanenko, M.A., Strom, S., Whitledge, T.E. 2010. Status and trends of the Bering Sea region, 2003-2008, pp 196-267 In S.M. McKinnell and M.J. Dagg [Eds.] Marine Ecosystems of the North Pacific Ocean, 2003-2008. PICES Special Publication 4, 393 p.

Hunter, K.A., Kim, J.P., Croot, P.L. 1997. Biological role of trace metals in natural waters. Environ. Monitor. Assess. 44, 103-147.

Ivanov, O.A. 1998. Epipelagic community of fishes and cephalopods in the Pacific Ocean off Kuril Islands in 1986-1995. TINRO 124: P. 3-54. (In Russian).

Katugin, O.N., Zuev, N.N. 2007. Distribution of cephalopods in the upper epipelagic northwestern Bering Sea in autumn. Reviews in Fish Biology and Fisheries 17(2-3): 283-294.

Khen, G.V. 2010. Hydrometeorological characteristic of the western Bering Sea, pp. 301-337, In. Makarevich, P.R. (Ed.) Current state of the ecosystem of the western Bering Sea, Southern Scientific Centre, Rostov-on-Don, Russia: 14-36. (In Russian).

Khen, G.V., Basyuk, E.O., Matveev, V.I. 2015. Parameters of the upper mixed layer and thermocline layer and chlorophyll-a in the western deep basin of the Bering Sea in summer and fall of 2002-2013. Izvestiya TINRO 182:115-131. (In Russian).

Khen, G.V., Basyuk, E.O., Zuenko, Yu.I., Ustinova, E.I., Figurkin, A.L., Shatilina, T.A. 2014. Hydrometeorological conditions in the Russian Far East Seas, 2012 and 2013. Fisheries Oceanography Issues. 11: 38-60. (In Russian).

Khoruzhiy, A.A. 2011. Features of species composition and abundance of nekton community in the upper epipelagic layer of the North-West Pacific in early summer season. Izvestia TINRO 164: 93-113. (In Russian).

Kivva, K.K., Kubriakov A.A. 2021. Seasonal and Interannual Variability of Chlorophyll-A Concentration in the Bering Sea Based on Satellite Data. Izvestiya, Atmospheric and Oceanic Physics 57(12): 1643–1657.

Klovach, N.V., El'nikov, A. N. 2013. Structure of Spawning School of Chum Salmon Oncorhynchus keta from Olutorsky Bay of the Bering Sea (Northeastern Kamchatka). Journal of Ichthyology 53(9): 720–730.

Kotenev, B.N. 1995. Water Dynamics as the principal Factor of long-term Variations of Bioproductivity and Reproduction of Fish Resources in the Bering Sea. In Comprehensive Studies of the Bering Sea Ecosystem. Moscow, Russian Federal Research Institute of Fisheries and Oceanography Publishers: 7–39. (In Russian).

Kotenev, B.N., Krovnin, A.S., Klovach, N.V., Mordasova, N.V., Muriy, G.P. 2015. Impact of climatic and oceanographic factors on the state of main pink salmon stocks, 1950–2015. Trudy VNIRO 158: 143-161. (In Russian).

Ladd, C. 2014. Seasonal and interannual variability of the Bering Slope Current. Deep Sea Research Part II: Topical Studies in Oceanography 109: 5-13.

Lane, T.W., Saito, M.A., George, G.N., Pickering, I.J., Prince, R.C., Morel, F.M.M. 2005. Biochemistry: a cadmium enzyme from marine diatom. Nature 435 (7038): 42.

Leblanc, K., Hare, C.E., Boyd, P.W., Bruland, K.W., Sohst, B., Pickmere, S., Lohan, M.C., Buck, K., Ellwood, M., Hutchins, D.A. 2005. Fe and Zn effects on the Si cycle and diatom community structure in two contrasting high and low-silicate HNLC areas. Deep Sea Research Part I: Oceanographic Research Papers 52(10): 1842-1864.

Loboda, S.V., Zhigalin, A.Yu. 2017. Some results of researches on pacific herring in the north western Bering Sea in 2010–2015. Izvestia TINRO 188: 125–139. (In Russian).

Lomas, M.W., Moran, S.B., Casey, J.R., Bell, D.W., Tiahlo, M., Whitefield, J., Kelly, R.P., Mathis, J.T. and Cokelet, E.D. 2012. Spatial and seasonal variability of primary production on the Eastern Bering Sea shelf. Deep Sea Research Part II: Topical Studies in Oceanography 65: 126-140.

Loughlin, T.R., Ohtani, K., 1999. Dynamics of the Bering Sea. University of Alaska Sea Grant.

Luchin, V.A. 2007. Seasonal variability of water temperature in the active layer of the Far Eastern seas. In Akulichev V.A. (Ed.), Far Eastern seas of Russia: in 4 books. Book 1. Oceanological studies. Nauka, Moscow, Russia: 232-253. (In Russian).

Luchin, V., Kruts, A., Sokolov, O., Rostov, V., Rudykh, N., Perunova, T., Zolotukhin, E., Pischalnik, V., Romeiko, L., Hramushin, V., Shustin, V., Udens, Y., Baranova, O., Smolyar, I., Yarosh, E. 2009. Climatic Atlas of the North Pacific Seas: Bering Sea, Sea of Okhotsk, and Sea of Japan. Akulichev, V., Volkov, Yu., Sapozhnikov, V., Levitus, S. (Eds.) Washington D.C.: U.S. Gov. Printing Office. 380 p. (CD).

Luchin, V.A., Sokolov, O.V., 2007. Interannual variability and forecast of the thermal condition in the upper layer in the Bering Sea. Izv. TINRO 151: 312-337.

Makarevich, P.R. (Ed.) 2010. Current state of the ecosystem of the western Bering Sea. Southern Scientific Centre, Rostov-on-Don, Russia. (in Russian).

Mamaev, E.G. 2018. A new method of counting *Phoca vitulina* ssp. *Stejnegeri* (Phocidae, Carnivora) on the Commander islands (Russia). Nature Conservation Research. Zapovednaya nauka 3(4): 44-58.

Matishov, G.G., Balykin, P.A., Karpenko, V.I. 2009. The large marine ecosystems of Russia: the western Bering Sea. Vestnik Uzhnogo nauchnogo centra RAS. 5(2). 49-57.

McKinnell, S.M., Dagg, M.J. (Eds.) 2010. Marine ecosystems of the North Pacific Ocean, 2003-2008. 393 p.

Moiseev, P.A. 1963. Some scientific prerequisites for the organization of the Bering Sea fishery research expeditions. In Soviet fisheries investigations in the North-Eastern part of the Pacific Ocean, Part 1. Moscow, Russia: 7-12. (In Russian).

Moore, G.W.K., Pickart, R.S. 2012. Northern Bering Sea tip jets. Geophysical Research Letters 39 (8): L08807.

Morel, F.M., Price, N.M. 2003. The biogeochemical cycles of trace metals in the oceans. Science 300(5621): 944-7.

Nadtochy, V.A., Kolpakov, N.V., Korneichuk, I.A., 2017. The distribution of macrozoobenthos taxa, as potential indicators of Vulnerable Marine Ecosystems in the Western Bering Sea: 1. Anadyr Bay area. Russian Journal of Marine Biology, 43(7): 555-567.

Nadtochy, V.A., Kolpakov, N.V. 2022. Macrozoobenthos of the Olyutorsky Bay (Bering Sea) a quarter of century later: composition, distribution, communities. Izvestiya TINRO 202(1): 161–171. (In Russian).

Natarov, V.V. 1963. On the water masses and currents of the Bering Sea. In Soviet fisheries investigations in the North-Eastern part of the Pacific Ocean, Part 1. Moscow, Russia: 111-134. (In Russian).

Naumenko, N.I. 2010. Dynamics of herring stock abundance Clupea pallasii Val. in the western Bering Sea. Issledovaniya vodnykh biologicheskikh resursov Kamchatki i severo-zapadnoj chasti Tikhogo okeana 16: 140-145. (In Russian).

Perry, R.I., McKinnell, S.M. (Eds.) 2004. Marine Ecosystems of the North Pacific. 280 p.

Pickart, R.S., Macdonald, A.M., Moore, G.W.K., Renfrew, I.A., Walsh, J.E. and Kessler, W.S. 2009. Seasonal evolution of Aleutian low pressure systems: Implications for the North Pacific subpolar circulation. Journal of Physical Oceanography 39(6): 1317-1339.

Radchenko, V.I. 1992. Role of squids in pelagic ecosystem of the Bering Sea. Oceanology 32(6): 1093-1101. (In Russian).

Roper, C.F.E., Young, R.E. 1975. Vertical distribution of pelagic cephalopods. Smithsonian contributions to zoology 209: 1-51.

Sambrotto, R.N., Niebauer, H.J., Goering, J.J., Iverson, R.L. 1986. Relationships among vertical mixing, nitrate uptake, and phytoplankton growth during the spring bloom in the southeast Bering Sea middle shelf. Continental Shelf Research 5(1-2): 161-198.

Savinykh, V. F. 1994. Migrations of Pacific pomfret. Biologia morya 4: 271-277. (In Russian).

Shuntov, V.P. 1988. Abundance and distribution of marine birds in the eastern part of the Far Eastern Russian EEZ in fall. 1. Marine birds in the Western Bering Sea. Zoologichesky Zhurnal 67(10): 1538-1548. (In Russian).

Shuntov, V.P. 2001. Biology of Far-Eastern Seas of Russia. Vol. 1. Vladivostok: TINRO-Center. 580 p. (In Russian).

Shuntov, V.P. 2016. Biology of Far Eastern Seas of Russia. Vol. 2. Vladivostok: TINRO-Center. 604 p. (In Russian).

Shuntov, V.P., Ivanov, O.A. 2015. Marine mammals in macro-ecosystems of the Far Eastern seas and adjacent waters of the North Pacific. Russian Journal of Marine Biology 41(7): 548-564.

Shuntov, V.P., Temnykh, O.S. 2011. Pacific salmon in marine and ocean ecosystems. Vol. 2 Vladivostok, TINRO. 473 p. (In Russian).

Shuntov, V.P., Volkov, A.F., Temnykh, O.S., Dulepova, E.P. 1993. Walley Pollock in the ecosystems of Far Eastern Seas. Vladivostok: TINRO. 426 p. (In Russian).

Somov, A.A. 2017. The Seasonal Dynamics of the Abundance and Species Composition of Nekton in the Upper Epipelagic Layer of the Western Bering Sea. Russian Journal of Marine Biology 43(7): 535-554.

Stabeno, P.J., Danielson, S.L., Kachel, D.G., Kachel, N.B. and Mordy, C.W. 2016. Currents and transport on the Eastern Bering Sea shelf: An integration of over 20 years of data. Deep Sea Research Part II: Topical Studies in Oceanography 134: 13-29.

Shevliakov, E.A., Dubinin, V.A., Bugaev, V.F., Zavarina, L.O., Feldman, M.G., Zakharova, O.A., Zikunova, O.V., Shubkin, S.V. 2016. Characteristics of coastal fishery of Pacific salmon in Kamchatka region in 2016. Bulletin of Pacific salmon studies in the Far East 11: 13-24. Vladivostok, Russia. (In Russian).

Shevliakov, E.A., Erokhin, V.G., Dubinin, V.A. 2009. Characteristics of coastal fishery of Pacific salmon in Kamchatka region. Bulletin of Pacific salmon studies in the Far East 4: 12-27. Vladivostok, Russia. (In Russian).

Shevliakov, E.A., Zavarina, L.O., 2004. On features of abundance dynamics and stock forecast methods of West Kamchatka chum salmon. Investigations of water living resources of Kamchatka and north-western part of the Pacific Ocean 7: 181-186. (In Russian).

Stepanenko, M.A., Gritsay, E.V. 2016. Assessment of stock, spatial distribution, and recruitment of walleye pollock in the northern and eastern Bering Sea. Izvestiya TINRO 185: 16-30. (In Russian).

Stepanenko, M.A., Gritsay, E.V. 2018. Environmental variability and spatial differentiation pollock in the Bering Sea. Trudy VNIRO 174: 6-20. (In Russian).

Takeda, S, Tsuda, A. 2005. An *in situ* iron-enrichment in the western subarctic Pacific (SEEDS): introduction and summary. Prog. Oceanogr. 64: 95-109.

Temnykh, O.S., Starovoytov, A.N., Glebov, I.I., Merzlyakov, A.Yu., Sviridov, V.V. 2003. Pacific salmon in the epipelagic fish communities of the south Okhotsk Sea. Izvestiya TINRO 132: 112-153. (In Russian).

Terziev, F.S. (Ed.). 1999. Hydrometeorology and Hydrochemistry of the seas. Project «Seas». Volume 10: Bering Sea, book 1: Hydrometeorological conditions. Saint-Petersburg, Russia, Gidrometeoizdat. 300 p.

Tortell, P.D., Price, N.M. 1996. Cadmium toxicity and zinc limitation in centric diatoms of the genius *Thalassiossira*. Mar. Ecol. Progr. Ser. 138: 245-254

Volkov, A.F. 1996. On methodology of sampling of zooplankton. Izvestiya TINRO 119: 306-311. (In Russian).

Volkov, A.F. 2008. Technique of collecting and processing the samples of plankton and the samples on nekton feeding (step-by-step instructions). Izvestiya TINRO 154: 405-416. (In Russian).

Volvenko, I.V., 2003. Morphometric characteristic of standard biostatistical regions for biocenologycal researches of Russian fishing zone on Far East. Izvestiya TINRO 132: 27-42. (In Russian).

Volvenko, I. V., 2021. A database of net zooplankton of the Far East seas and adjacent Pacific Ocean waters, Earth Syst. Sci. Data Discuss. [preprint], https://doi.org/10.5194/essd-2021-29. 34 p.

Urawa, S., Sato S., Crane, P.A., Agler, B., Josephson, R., Azumaya, T. 2009. Stock-specific ocean distribution and migration of chum salmon in the Bering Sea and North Pacific Ocean. N. Pac. Anadr. Fish Comm. Bull. 5: 131-146.

Watanabe, H., Kubodera, T., Moku, M., Kawaguchi, K. 2006. Diel vertical migration of squid in the warm core ring and cold water masses in the transition region of the western North Pacific. Marine Ecology Progress Series 315: 187-197.

Wcislo, E., Loven, D., Kucharski, R., Szdzuj, J. 2008. Human health risk assessment, case study: An abandoned metal smelter site in Poland. Chemosphere 96: 223-230.

Zavarina, L.O. 2008. Biology and dynamics of chum salmon (*Oncorhynchus keta*) population at the northeastern coast of Kamchatka. Cand. Sci. (Biol.) Dissertation, VNIRO, Moscow, Russia. (In Russian).

Zavolokina, E.A., Zavolokin, A.V. 2007. Distribution, abundance, age and size composition of chum salmon in the western Bering Sea and adjacent Pacific in 2002-2006. Izvestiya TINRO 151: 35-60. (In Russian).